Liu *et al. BMC Biology* (2024) 22:159
https://doi.org/10.1186/s12915-024-01959-1

BMC Biology

RESEARCH ARTICLE

Hierarchical lncRNA regulatory network in early-onset severe preeclampsia

Haihua Liu[1,2,3,4,5,6†], Zhijian Wang[1,2,3,4†], Yanjun Li[1,2,3,4,5,6†], Qian Chen[2], Sijia Jiang[2], Yue Gao[1,2,3,4,5,6], Jing Wang[1,2,3,4,5,6], Yali Chi[1,2,3,4,5,6], Jie Liu[2], Xiaoli Wu[2], Qiong Chen[2], Chaoqun Xiao[2], Mei Zhong[2], Chunlin Chen[2*] and Xinping Yang[1,2,3,4,5,6,7*]

Abstract

Background Recent studies have shown that several long non-coding RNAs (lncRNAs) in the placenta are associated with preeclampsia (PE). However, the extent to which lncRNAs may contribute to the pathological progression of PE is unclear.

Results Here, we report a hierarchical regulatory network involved in early-onset severe PE (EOSPE). We have carried out transcriptome sequencing on the placentae from patients and normal subjects to identify the differentially expressed genes (DEGs), including some lncRNAs (DElncRNAs). We then constructed a high-quality hierarchical regulatory network of lncRNAs, transcription factors (TFs), and target DEGs, containing 1851 lncRNA-TF interactions and 6901 TF-promoter interactions. The lncRNA-to-target regulatory interactions were further validated by the triplex structures between the DElncRNAs and the promoters of the target DEGs. The DElncRNAs in the regulatory network were clustered into 3 clusters, one containing DElncRNAs correlated with the blood pressure, including *FLNB-AS1* with targeting 27.89% (869/3116) DEGs in EOSPE. We further demonstrated that *FLNB-AS1* could bind the transcription factor JUNB to regulate a series members of the HIF-1 signaling pathway in trophoblast cells.

Conclusions Our results suggest that the differential expression of lncRNAs may perturb the lncRNA-TF-DEG hierarchical regulatory network, leading to the dysregulation of many genes involved in EOSPE. Our study provides a new strategy and a valuable resource for studying the mechanism underlying gene dysregulation in EOSPE patients.

Keywords Preeclampsia, Long non-coding RNA, Hierarchical regulatory network, *FLNB-AS1*, HIF-1 signaling pathway

[†]Haihua Liu, Zhijian Wang, Yanjun Li contributed equally to this work.

*Correspondence:
Chunlin Chen
ccl1@smu.edu.cn
Xinping Yang
xpyang1@smu.edu.cn
[1] Center for Genetics and Developmental Systems Biology, Nanfang Hospital, Southern Medical University, Guangzhou 510515, China
[2] Department of Obstetrics & Gynecology, Nanfang Hospital, Southern Medical University, Guangzhou 510515, China
[3] State Key Laboratory of Organ Failure Research, Division of Nephrology, Nanfang Hospital, Southern Medical University, Guangzhou 510515, China
[4] Department of Bioinformatics, School of Basic Medical Sciences, Southern Medical University, Guangzhou 510515, China
[5] Key Laboratory of Mental Health of the Ministry of Education, Guangdong-Hong Kong-Macao Greater Bay Area Center for Brain Science and Brain-Inspired Intelligence, School of Basic Medical Sciences, Southern Medical University, Guangzhou 510515, China
[6] Guangdong Key Laboratory of Psychiatric Disorders, School of Basic Medical Sciences, Southern Medical University, Guangzhou 510515, China
[7] Department of Psychology, School of Public Health, Southern Medical University, Guangzhou 510515, Guangdong, China

Background

Preeclampsia (PE) is a pregnancy complication with hypertension presenting after 20 weeks of gestation, usually with signs of damage to other maternal organs such as the liver and kidney [1]. The global incidence rate is 4.6% of pregnancies [2], leading to 60,000 maternal deaths yearly [3]. PE has grave consequences on both maternal health and fetal development. It is believed that placentae from PE patients produce factors that mediate abnormal autonomic nervous system functions [4–6], leading to cerebral edema, intracranial hemorrhage, and eclampsia [7, 8]. The abnormal function of the preeclamptic placentae can also cause perinatal and infant morbidity or mortality [9], preterm births [10], and fetal growth restriction (FGR) [11, 12]. In the long term, PE affects the development and functions of the brain [13], leading to intellectual disability [14], epilepsy [15], autism [16–18], and schizophrenia [19, 20] in the offspring. Because the mechanism underlying this disease remains unknown, neither effective therapies nor early diagnoses are available. Therefore, a systematic search for pathogenic molecular pathways is in urgent need.

The root cause of PE is believed to be in the placenta, and therefore identification of the factors that affect the development of the placenta has been the focus of recent studies. Researchers have been searching for genes that confer the susceptibilities of this disease. However, most of the efforts have been focused on protein-coding genes [21–23] until recently when accumulating lines of evidence have shown that long non-coding RNAs (lncRNAs) are essential regulators of cellular functions in different tissues and diseases [24–29]. It has been known that lncRNAs are extensively reported to be involved in transcriptional regulation [30]. One of the significant functions of lncRNAs is to interact with transcription factors (TFs) or chromatin remodeling factors (CRFs), facilitating or inhibiting their binding or activity at targeted DNA regions [31], such as *linc-YY1* interacting with transcription factor YY1 [32]. In addition, lncRNA can bind with one of the DNA strands or duplex DNA to guide the proteins to the targeted regions [33, 34]. Some lncRNAs, such as *HOTAIR* [35], *MEG3* [36], *SPRY4-IT1* [37], *TUG1* [38], and *MALAT1* [39], have been reported to be involved in the invasion and migration of placental trophoblast cells, which are crucial for placenta development. We have recently identified about four hundred differentially expressed lncRNAs, among a total number of more than three thousand differentially expressed genes (DEGs), in the placentae of PE patients [40]. Yet, we do not know if and to what extent these lncRNAs may contribute to this disease. Therefore, we hypothesized that many of these DElncRNAs may actively regulate the transcription of genes in the placenta of PE patients, leading to the differential expression of a large number of genes.

Among the identified DElncRNAs, we have picked two DElnRNAs (*SH3PXD2A-AS1* and *INHBA-AS1*) to study their regulation on the activity of transcription factors and their involvement in the proliferation and invasion of trophoblast cells [41, 42], which support our hypothesis about the DElncRNAs in the regulation of the placental gene transcription. Here, we report our systematic search for lncRNAs that may contribute to the changed gene expression in the placentae of PE patients via the construction of a high-quality lncRNA-TF-DEG hierarchical regulatory network. We built this lncRNA regulatory network by searching DElncRNA-TF interactions and TF-binding motifs in the promoters of DEGs and obtained a network containing 1,851 DElncRNA-TF interactions and 6901 TF-DEG interactions. We further controlled the quality of the network by searching the triplex structures between the DElncRNAs and the promoters of DEGs, removing the edges not supported by the triplex structures. We performed hierarchical clustering analysis for DElncRNAs based on the similarity of their targets and obtained three functional clusters. One of the three clusters was tightly associated with EOSPE. In this cluster, all DElncRNAs were correlated well with the patient's blood pressure, showing much higher AUC and correlation than the DElncRNAs of the other two clusters. To further verify our method of searching for PE-associated DElncRNAs, we carried out a functional investigation on *FLNB-AS1*, one of the DElncRNAs in this cluster, which targets 27.89% (869/3116) DEGs in EOSPE. We demonstrated that *FLNB-AS1* could bind the transcription factor JUNB to regulate a series of members of the HIF-1 signaling pathway in trophoblast cells. We thus identified a regulatory pathway *FLNB-AS1*/JUNB/HIF-1 axis, which was consistent with the reported placental hypoxia hypothesis in PE [43, 44]. These results suggest that the DElncRNAs may contribute to most of the gene dysregulation in the placentae of EOSPE, and therefore, the DElncRNA hierarchical regulatory network would provide a rich resource for further study on the molecular mechanisms underlying EOSPE.

Results

Differentially expressed lncRNAs in the placental transcriptome of early-onset severe preeclampsia

We have previously carried out transcriptome sequencing on the placentae from PE patients (EOSPE: $n=9$; LOSPE: $n=15$; LOMPE: $n=9$) and normal subjects ($n=32$) and identified about three thousand differentially expressed genes (DEGs), including about four hundred differentially expressed lncRNAs (DElncRNAs) [40]. Since most of the DEGs were found

in EOSPE, we decided to systematically investigate if and how the DElncRNAs were involved in such a large-scale differential expression in the placentae of EOSPE patients. We revisited the transcriptome data of the placentae, focusing on EOSPE ($n=9$) and normal ($n=32$) subjects (Additional file 1: Table S1), and identified 3116 DEGs, including 2536 protein-coding genes, 383 lncRNAs, and 197 other genes (Additional file 2: Fig. S1A, Additional file 1: Table S2, FDR < 0.05). We wanted to know if these 383 lncRNAs are involved in the pathogenesis of EOSPE and to what extent these lncRNAs may contribute to the differential gene expression in EOSPE. Of the 383 DElncRNAs, 146 were upregulated, and 237 were downregulated (Fig. 1A). Quantitative RT-PCRs were performed to validate the expression changes of some DElncRNAs (Fig. 1B, Additional file 2: Fig. S1B, Additional file 1: Table S3 and Table S4).

We assessed the correlation between the DElncRNAs and the blood pressure of the individuals (patients and normal controls) and found that 57.44% (220/383) of the DElncRNAs were correlated with systolic pressure, 60.31% (231/383) of the DElncRNAs were correlated with diastolic pressure (Fig. 1C). For example, *FLNB-AS1*, *MIR193BHG*, *MYCNUT*, and *AC110619.1* were positively correlated with blood pressure, whereas *AL121839.2* was negatively correlated with blood pressure (Fig. 1D, Additional file 2: Fig. S1C). Therefore, the expression levels of these DElncRNAs were further used to discriminate EOSPE patients from normal pregnant individuals using receiver operating characteristic (ROC) curves analysis, and the area under the curve (AUC) was used as the effective measure of accuracy (see "Methods"). The discrimination accuracy of DElncRNAs was higher than coding DEGs (Fig. 1E, $p=2.808e-16$, Wilcoxon test), and the AUC of *FLNB-AS1*, *MIR193BHG*, *MYCNUT*, *AC110619.1*, and *AL121839.2* were higher than 0.885 (Fig. 1F, Additional file 2: Fig. S1D). These results show a clear association between DElncRNAs and the primary symptom of EOSPE.

DElncRNAs are involved in PE-related functions

LncRNAs often exert their functions by interacting with molecules, such as proteins, DNAs, and RNAs [45, 46], and therefore their functions can be deduced from their interacting partners. We collected RNA–protein interaction data from starBase (v3.0) [47], RNAct [48], RNAinter (v4.0) [49], and NPInter (v5.0) [50] (Additional file 3: Table S1). We obtained 97,255 interactions between 383 DElncRNAs and 3790 proteins and constructed a DElncRNA-protein interaction network (DElncRNA-Prot Network) (Fig. 2A). In addition, the DElncRNA-interacting proteins are enriched with PE candidate genes (Fig. 2B) and DEGs in EOSPE (Fig. 2C), suggesting that DElncRNA-Prot Network may be involved in EOSPE.

To explore the associated pathways and molecular functions of DElncRNAs, we performed enrichment analyses on the Kyoto Encyclopedia of Genes and Genomes (KEGG) and Gene Ontology (GO) terms for the proteins interacting with DElncRNAs (Additional file 4: Fig. S2A-D, Additional file 3: Table S2-S3). Most of the enriched KEGG pathways were involved with human disease, immune system, cell growth and death, and gene regulation, 16 (30.77%, 16/52) of which were cancer pathways (Additional file 4: Fig. S2A). The enriched GO biological process (GO BP) terms were also associated with regulating the cell cycle, immune response, and gene regulation (Additional file 4: Fig. S2B). These enriched functions are consistent with previous studies on the mechanism of PE and point to impaired placental development, inadequate proliferation, and poor trophoblast invasion [38, 51–55]. Furthermore, the enriched GO cellular component (GO CC) terms were associated with transcription regulator complex (Additional file 4: Fig. S2C), and the enriched GO molecular function (GO MF) terms were associated with DNA-binding transcription factor binding (Additional file 4: Fig. S2D), suggesting that DElncRNAs may regulate gene expression through interacting transcription regulators. Indeed, we found that 12.37% (469/3790) DElncRNA-interacting proteins were transcription factors (TFs), showing significant enrichment compared with 6.27% (1009/16,088) in the expressed genes (Fig. 2D,

(See figure on next page.)

Fig. 1 Differentially expressed lncRNAs (DElncRNAs) in the placentae of EOSPE patients. **A** The expression pattern of 383 DElncRNAs (237 downregulated and 146 upregulated) across 41 samples (9 EOSPE samples and 32 normal samples). The bars on top indicate 5 aspects of the subjects: (1) sample groups: EOSPE (red) and normal (navy blue); (2) blood pressure: systolic pressure (dark green) and diastolic pressure (blue); (3) age of the mother: purple; (4) gestation days (pink); (5) baby weight (red). **B** The relative expression levels of *FLNB-AS1* (EOSPE $n=8$, Normal $n=6$, Student's *t* test), *MIR193BHG* (EOSPE $n=8$, Normal $n=9$, Student's *t* test), *MYCNUT* (EOSPE $n=7$, Normal $n=8$, Wilcoxon test), *NAV2-AS4* (EOSPE $n=7$, Normal $n=7$, Student's *t* test), and *CYP1B1-AS1* (EOSPE $n=7$, Normal $n=7$, Student's *t* test) measured by qRT-PCR. **C** The number of DElncRNAs significantly correlated with blood pressure. **D** Spearman's correlation between blood pressure and the expression levels of *FLNB-AS1*, *MIR193BHG*, and *MYCNUT* based on RNA-seq data. Blue indicates systolic pressure, red indicates diastolic pressure, the circle indicates EOSPE samples, and the triangle indicates normal samples. TPM: transcripts per million. **E** The distribution of AUC between coding DEGs and DElncRNAs. The *p*-value was calculated using a two-sided Wilcoxon test. **F** The discrimination accuracy of *FLNB-AS1*, *MIR193BHG*, and *MYCNUT*

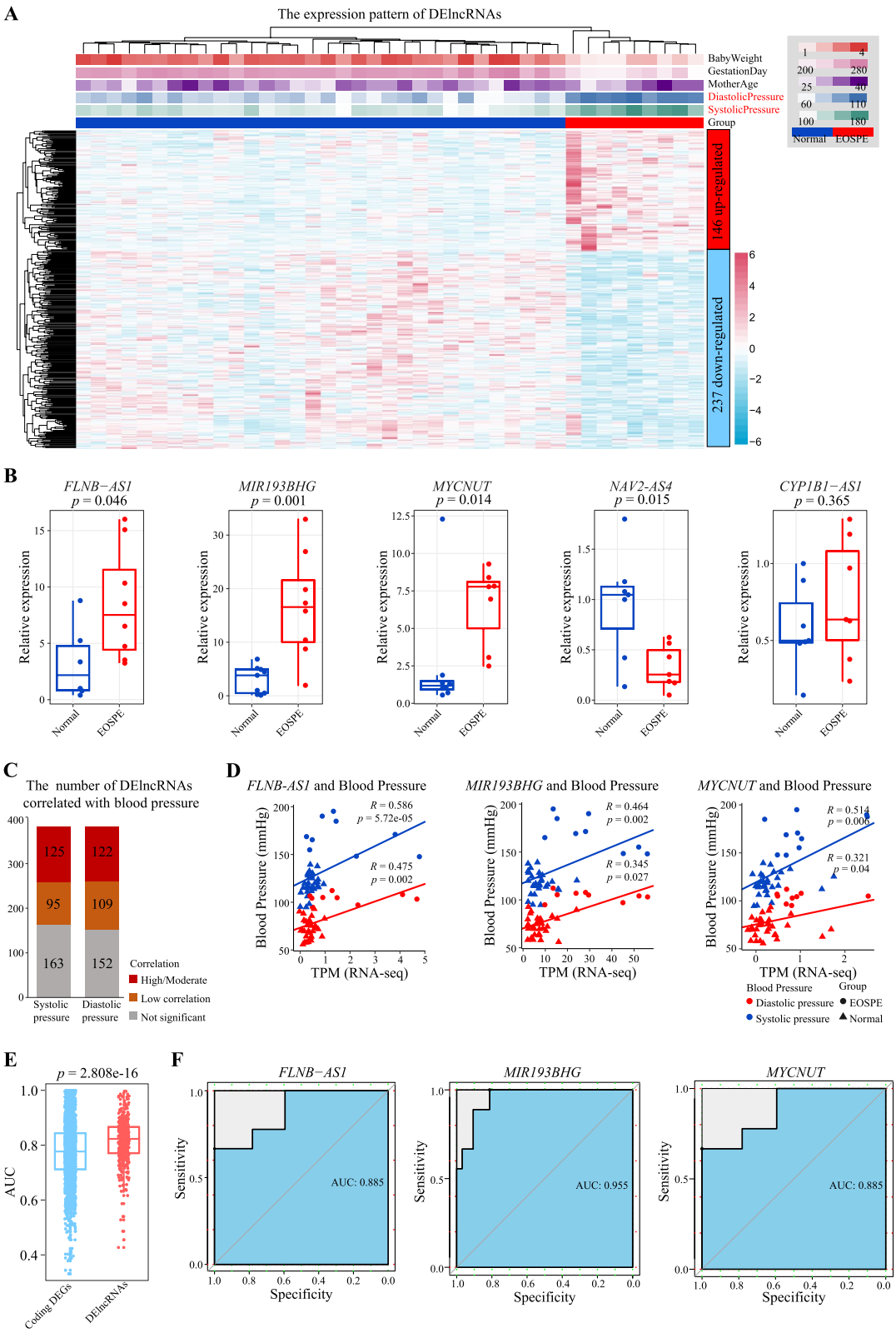

Fig. 1 (See legend on previous page.)

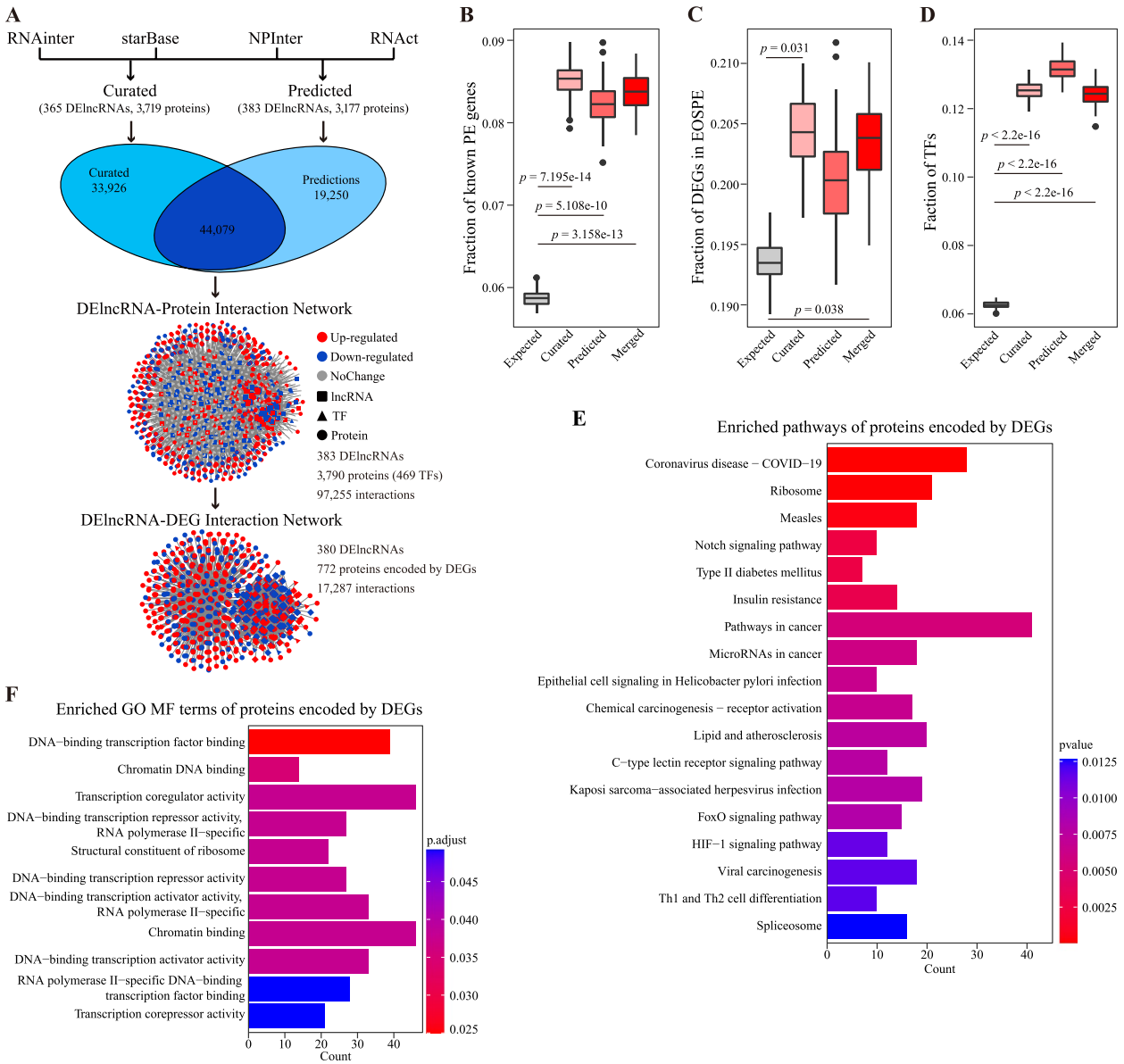

Fig. 2 Proteins interacting with DElncRNAs are involved in the cellular functions associated with PE. **A** Flowchart for the construction of DElncRNA-protein interaction network. The rectangle indicates lncRNAs, the triangle indicates transcription factors, and the circle indicates proteins. Red indicates upregulated genes in EOSPE, blue indicates downregulated genes in EOSPE, and grey indicates genes with no significant change in EOSPE. **B–D** DElncRNA interactors are enriched with PE-related genes from literature (**B**); DElncRNA interactors are enriched with DEGs in EOSPE (**C**); DElncRNA interactors are enriched with transcription factors (**D**). The fraction variation was estimated using a bootstrapping method with 100 resamplings, and the *p*-value was calculated by a one-sided Fisher's exact test. **E** The enriched KEGG pathways of DEGs in the network. **F** The enriched GO MF terms of DEGs in the network

Additional file 4: Fig. S2E, $p < 2.2e-16$, Fisher's exact test, Additional file 3: Table S1). In the DElncRNA-Prot Network, 98.69% (378/383) DElncRNAs showed physical interaction with TF, and proteins interacting with 334 DElncRNAs were enriched with TFs (Additional file 3: Table S7), such as *INHBA-AS1*, *FLNB-AS1*, and *SH3PXD2A-AS1* (Additional file 4: Fig. S2F).

We retrieved the DElncRNA-DEG interaction network (DElncRNA-DEG Network) (Fig. 2A) from the DElncRNA-Prot Network. To explore the associated pathways and molecular functions of DElncRNAs in EOSPE, we performed enrichment analyses on the KEGG and GO MF terms for the DEGs interacting with DElncRNAs (Fig. 2E–H, Additional file 3: Table S4-S6). We got 18

enriched pathways, some of which have been reported in previous studies, such as spliceosome [56], Th1 and Th2 cell differentiation [57], HIF-1 signaling pathway [58–60], FoxO signaling pathway [61, 62], pathways in cancer [58], insulin resistance [61], notch signaling pathway [63, 64], and ribosome [56, 65] (Fig. 2E), suggesting that these DElncRNAs may contribute to the disease through interacting with proteins encoded by DEGs in the patients. Moreover, we found 11 enriched GO MF terms for the DEGs interacting with DElncRNAs, which were mainly associated with gene regulation, such as DNA-binding transcription factor binding, chromatin DNA binding, and transcription coregulator activity (Fig. 2F). These enriched molecular function terms are consistent with the enrichment of TFs in the network, suggesting that transcription regulation may be the primary function of the DElncRNAs.

DELncRNAs interact with transcription factors predicted to regulate differential expression

We used HOMER to search for TF-binding motifs for the DEGs. We got 18 enriched TF-binding motifs with corresponding TFs, which were expressed in the placentae (Fig. 3A, Additional file 5: Table S1 and Table S2), including four TFs (USF2, FOSL1, FOSL2, and HIF1A) for upregulated genes, five TFs (MEF2A, TGIF1, PBX2, ZEB2, and TCF3) for downregulated genes, and 9 TFs for both upregulated and downregulated genes (Fig. 3A). Four of these TFs were themselves differentially expressed in EOSPE, including 3 upregulated TFs (ATF3, FOSL2, and MEF2A) and 1 downregulated TF (BATF) (Additional file 6: Fig. S3A). However, these 4 dysregulated TFs only target 917 (29.43%) DEGs based on the TF-binding motifs in the promoter regions (Additional file 6: Fig. S3B). Therefore, the DElncRNAs might be responsible for most differential transcription in EOSPE through a mechanism involving lncRNA-TF interaction.

These 18 TFs target 79.55% (2479/3116) of all DEGs (Fig. 3B), and 17 of 18 TFs interact with 346 of the 383 DElncRNAs (Additional file 3: Table S1), suggesting that DElncRNAs may be among the key factors responsible for the differential expression of genes found in EOSPE. A potential mechanism for lncRNAs to regulate gene expression is to scaffold TF-promoter complexes by forming lncRNA-DNA triplex structures [33, 66] (Fig. 3C, up) or compete with TF for transcription factor binding sites in the promoters [67] (Fig. 3C, bottom). We characterized the triplex-forming potential between 383 DElncRNAs and the promoter regions of 3116 DEGs using TDF (Triplex Domain Finder) (see "Methods") [68]. Of the 383 DElncRNA, 78.72% (290/383) were likely to form 3,513,560 triplex structures with significant DNA binding domains (DBD) in the promoter regions of 84.98% (2648/3116) DEGs (Additional file 7: Table S1). Furthermore, of the 2479 DEGs regulated by TFs, 95.08% (2357/2479) were predicted to form triplex structures between their promoters and the DElncRNAs, showing the significant enrichment (Fig. 3D, Fisher's exact test, $p < 2.2e-16$). In addition, we calculated the Pearson's correlation between DElncRNAs and DEGs (FDR < 0.05, Additional file 8: Table S1) and found that DEGs co-expressed with DElncRNAs were significantly enriched with DEGs targeted by the 18 TFs (Fig. 3E, Fisher's exact test, $p = 0.0034$), and also with DEGs whose promoters predicted to form triplex with DElncRNAs (Fig. 3F, Fisher's exact test, $p = 0.0056$).

We constructed a DElncRNA-TF-DEG network by integrating a curated DElncRNA-TF interaction network and TF-target regulatory network, then filtering with DElncRNA-promoter interactions and DElncRNA-DEG co-expression (Additional file 9: Fig. S4A-B). The DElncRNA-TF-DEG network contains 51,031 DElncRNA-promoter interactions, involving 252 DElncRNAs, 17 TFs, 2039 DEGs, 2531 DElncRNA-TF interactions, and 6914 TF-promoter interactions (Additional file 9: Fig.

(See figure on next page.)

Fig. 3 Construction of DElncRNA-TF-DEG hierarchical regulatory network reveals pathways dysregulated by the DElncRNAs. **A** The 18 significant TF-binding motifs predicted by HOMER are based on three sets of genes: upregulated genes, downregulated genes, and all DEGs. The number inside the parentheses indicates the number of TF-targeted DEGs. **B** Of 3116 DEGs in EOSPE, 79.56% (2479/3116) are predicted targets of the 18 TFs. **C** Schematic of the lncRNA-DNA triplex structures: The lncRNA recruits TFs to the promoters (i); lncRNA competes with TF for transcription factor binding sites (TFBSs) (ii). The interactions within the triplet structure include lncRNA-TF interaction, lncRNA-promoter triplex, and TF-promoter interaction. **D** The DEGs with binding motifs of the 18 TFs and binding sites of the 290 DElncRNAs. Left: the overlaps of DEGs with the TF-binding motifs and DElncRNA binding sites. Right: The DEGs with DElncRNA binding sites are enriched with TF-targeted DEGs. One-tailed Fisher's exact test is used to calculate the *p*-value. The fraction variation was estimated using a bootstrapping method with 100 resamplings. **E,F** The DEGs co-expressed with DElncRNAs are enriched with DEGs with the TF-binding motifs (79.46%, 2476/3107) (**E**) and DEGs with DElncRNA binding sites (85.10%, 2644/3107) (**F**). One-tailed Fisher's exact test was used to calculate the *p*-values. The fraction variation was estimated using a bootstrapping method with 100 resamplings. **G** The core DElncRNA-TF-DEG hierarchical regulatory network contains 169 DElncRNAs, 17 TFs, and 2037 DEGs. The rectangle indicates lncRNAs, the triangle indicates transcription factors, and the circle indicates DEGs targeted by DElncRNAs and TFs. Red indicates genes upregulated in EOSPE, blue indicates genes downregulated in EOSPE, and grey indicates genes with no significant change in EOSPE. **H** The enriched KEGG pathways of DEGs in the core DElncRNA-TF-DEG hierarchical regulatory network

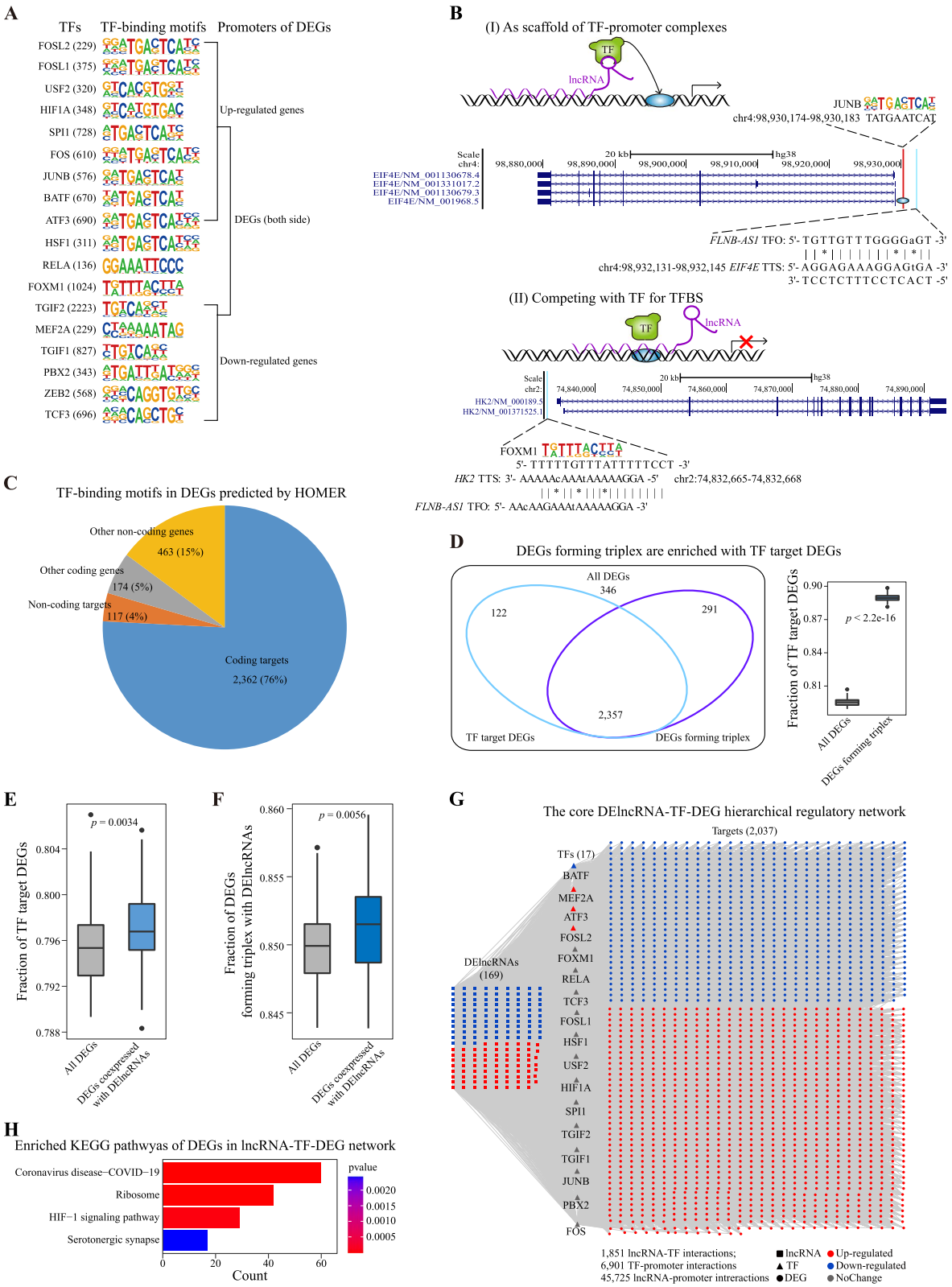

Fig. 3 (See legend on previous page.)

S4A-B, Additional file 10: Table S1). As described above, the lncRNA may serve as a scaffold between TFs and promoters. For each DElncRNA in the DElncRNA-TF-DEG network, we calculated the enrichment of lncRNA-targeted DEGs (whose promoters interact with the lncRNA and the expression levels are also significantly correlated with the lncRNA) in the TF-targeted DEGs (whose promoters harbor the binding sites of the TFs). We found 67.06% (169/252) DElncRNAs with significant enrichment (Additional file 10: Table S2). These 169 DElncRNAs may more likely regulate gene expression by serving as scaffolds between TF and promoter regions. Based on these DElncRNAs and their scaffolded TF-promoter interactions, we obtained a high-quality core DElncRNA-TF-DEG network containing 169 DElncRNAs (44.12% of all DElncRNAs), 17 TFs, and 2037 DEGs (65.37% of all DEGs), 1851 DElncRNA-TF interactions, 6901 TF-promoter interactions, and 45,725 DElncRNA-promoter interactions (Fig. 3G). We performed KEGG enrichment analyses on DEGs in the hierarchical regulatory network and found 4 enriched pathways, 3 of which were also enriched in all DEGs in EOSPE, including ribosome, coronavirus disease—COVID-19, and HIF-1 signaling pathway (Fig. 3G, Additional file 3: Table S6 and Additional file 10: Table S3). The ribosome [56, 65] and HIF-1 signaling pathway [58–60] have been recurrently reported in previous studies. These results suggest that DElncRNAs may interact with TFs to alter gene expression.

A group of lncRNAs associated with the main clinical symptom of PE

The "DElncRNA-TF-DEG" is a densely connected network, in which one lncRNA can recruit multiple TFs and target multiple promoters and one promoter can be targeted by multiple lncRNAs and TFs (Fig. 3G), showing a coordinate regulatory relationship. We performed the hierarchical clustering analysis for DElncRNAs and grouped them into 3 clusters (Fig. 4A, Additional file 11: Table S1 and Table S2, see "Methods"). The expression levels of the DElncRNAs in cluster 1 (C1) and cluster 2 (C2) are significantly correlated with blood pressure (Fig. 4B, E, Additional file 12: Fig. S5A). The AUC of DElncRNAs in C1 is significantly higher than all DElncRNAs in the hierarchical regulatory network (Fig. 4C, Wilcoxon test), and the correlation between DElncRNAs in C1 and blood pressure is stronger than all DElncRNAs in the network (Fig. 4D, Wilcoxon test). Cluster 1 has 48 DElncRNAs: 36 upregulated lncRNAs and 12 downregulated lncRNAs (Fig. 4E). Some DElncRNAs have been previously reported to associate with PE: *MIR193BHG* [69], *EGFR-AS1* [70], *GATA3-AS1* [71], *TCL6* [72], and *WDR86-AS1* [73]. We have recently found that *SH3PXD2A-AS1* [41] and *INHBA-AS1* [42] recruit TF to the DEG promoters in EOSPE, inhibiting the invasion and migration of trophoblast cells. These results suggest that the 48 DElncRNAs in C1 may be the leading group of lncRNAs that contribute to the pathogenesis of EOSPE.

To explore the associated pathways of each DElncRNA, we performed functional enrichment analyses on the DEGs target by each lncRNA in C1 and found 58 enriched KEGG pathways (Fig. 4F, Additional file 11: Table S3). Most enriched pathways involved signal transduction, such as the HIF-1 signaling pathway, PI3K-Akt signaling pathway, FoxO signaling pathway, Toll-like receptor signaling pathway, and AMPK signaling pathway (Fig. 4F, Additional file 11: Table S3). Many of them are reported to be associated with PE in previous studies. For example, the HIF-1 signaling pathway [59, 74], galactose metabolism [75, 76], and ribosome [56, 65] have been documented to be associated with PE. Of the 48 DElncRNAs, 30 (62.5%) are involved in the HIF-1 signaling pathway, e.g., *FLNB-AS1* and *MIR193BHG* (Fig. 4F). Most of the DEGs in the HIF-1 signaling pathway are associated with blood pressure (Additional file 12: Fig. S5B). For example, the upregulation of *FLT1* (Fms-Like Tyrosine Kinase 1) and HK2 are well-correlated with blood pressure. *FLT1* is a biomarker of EOSPE [77, 78]. HK2 is also reported to be involved in the pathogenesis of PE [79]. Sixteen of the 48 DElncRNAs (33.33%) are involved in galactose metabolism (Fig. 4F, Additional

(See figure on next page.)

Fig. 4 Modularity analysis of the core DElncRNA-TF-DEG network reveals a group of lncRNAs significantly correlated with the blood pressure of EOSPE patients. **A** The DElncRNAs clustering heatmap according to the similarity of DEGs and grouped DElncRNAs into 3 clusters. Each row and column represents a DElncRNA. **B** DElncRNAs in clusters 1 (C1) and 2 (C2) were enriched with those lncRNAs associated with blood pressure. One-tailed Fisher's exact test was used to calculate the *p*-values. The fraction variation was estimated using a bootstrapping method with 100 resamplings. **C** The AUC of DElncRNAs in C1 was significantly higher than the AUC of all DElncRNAs and DElncRNAs in hierarchical regulatory network. The *p*-values were calculated using a two-sided Wilcoxon test. **D** The correlation between DElncRNAs in C1 and blood pressure was significantly stronger than the correlation between all DElncRNAs/DElncRNAs in hierarchical regulatory network and blood pressure. The *p*-values were calculated using a two-sided Wilcoxon test. **E** The heatmap shows the significance between DElncRNAs in C1 and blood pressure, and the bar plot shows the absolute log2FoldChange of DElncRNAs. Red indicates the upregulated DElncRNAs, and blue indicates the downregulated DElncRNAs. *** $p < 0.001$, ** $p < 0.01$, * $p < 0.05$. **F** The Sankey plot shows the DEGs regulated by DElncRNAs in C1 and the significant pathways with adjusted *p*-value < 0.05

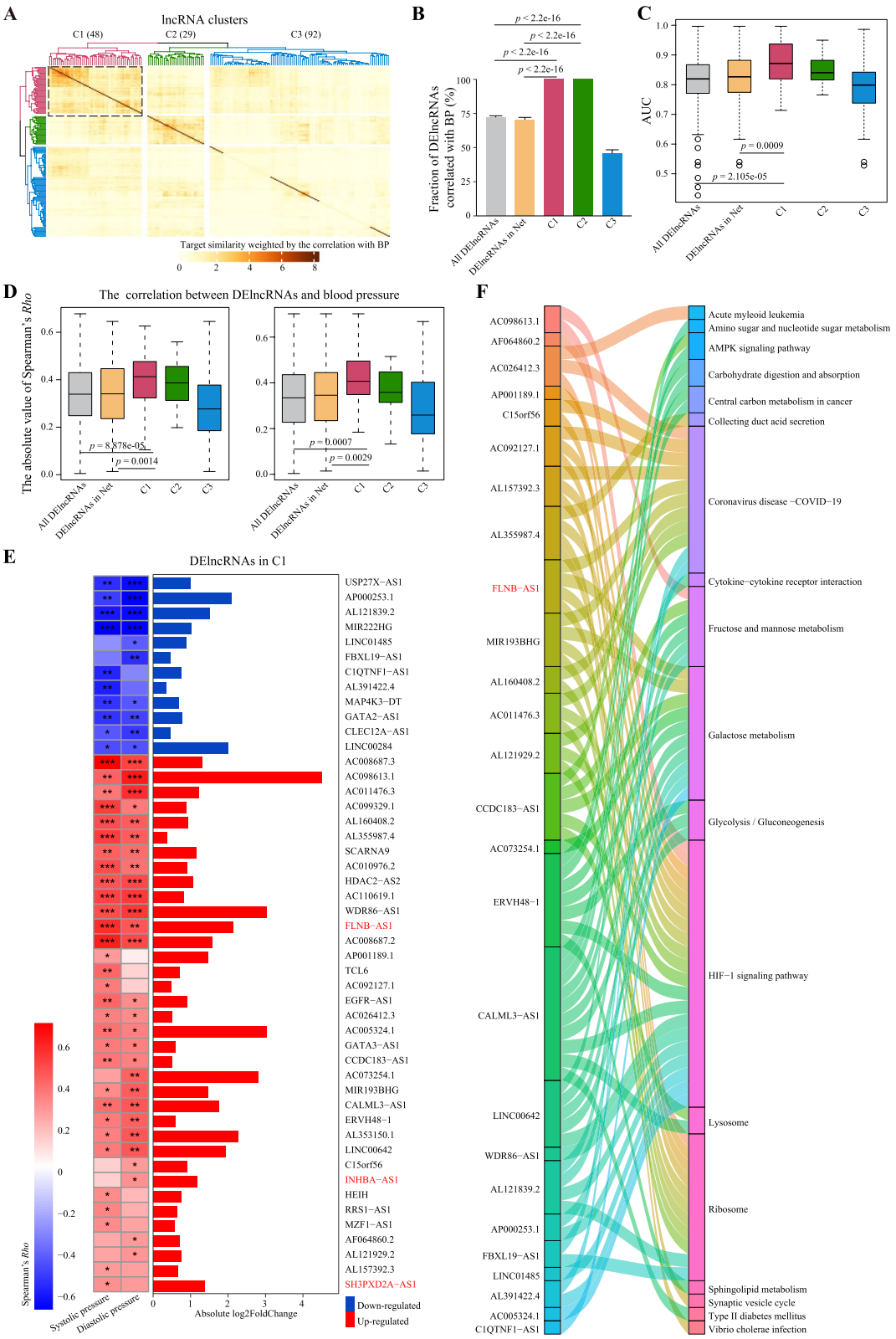

Fig. 4 (See legend on previous page.)

file 11: Table S3), with 9 targeted DEGs (7 upregulated genes and 2 downregulated genes). Many of the targeted DEGs are correlated with blood pressure (Additional file 12: Fig. S5C). Fourteen (14/48 = 29.17%) DElncRNAs are involved in the ribosome pathway (Fig. 4F, Additional file 11: Table S3), with 42 targeted DEGs (40 upregulated genes and 2 downregulated genes). Also, many of the targeted DEGs are correlated with blood pressure (Additional file 12: Fig. S5D).

FLNB-AS1-JUNB-HIF-1 *axis* in EOSPE

As described above, the DElncRNAs in C1 may be the leading group of lncRNAs that contribute to the pathogenesis of EOSPE. We ranked the lncRNAs in cluster 1 according to their importance in the hierarchical network (number of targeted DEGs and the *p*-value of DElncRNA as scaffold for TF-promoter interactions) and their association with blood pressure (the *p*-value of Spearman correlation with systolic pressure, the *p*-value of Spearman correlation with diastolic pressure) and the number of targeted DEGs involved in HIF-1signaling pathway (Additional file 11: Table S4). *FLNB-AS1* is at the top of this rank. Therefore, we chose *FLNB-AS1* to do the further experiments.

In the hierarchical regulatory network, *FLNB-AS1* interacts with 14 TFs (including SPI1, ATF3, BATF, FOS, FOXM1, HSF1, JUNB, RELA, FOSL2, FOSL1, HIF1A, USF2, TCF3 and MEF2A) to regulate 869 DEGs in EOSPE (Additional file 10: Table S1). The targets of the DElncRNA *FLNB-AS1* were significantly enriched with the HIF-1 signaling pathway members, a pathway reported to be involved in PE [59, 77]. As expected, the lncRNA *FLNB-AS1* is mainly in the nucleus (Fig. 5A, Additional file 13: Table S1). In addition, we conducted RNA antisense purification (RAP) followed by mass spectrometry to determine proteins interacting with *FLNB-AS1* and detected 500 proteins interacting with *FLNB-AS1*, including 27 TFs (Fig. 5B, Additional file 13: Table S2-S4). Of the 27 TFs, only JUNB was predicted as a critical TF-driven gene expression change in EOSPE (Fig. 3A).

As described above (Fig. 3A), JUNB has binding motifs in the promoters of 576 DEGs. Most interestingly, 252 of 576 DEGs are correlated with systolic blood pressure, and 282 of 576 DEGs are correlated with diastolic blood pressure (Fig. 5C). These DEGs are significantly enriched in the HIF-1 signaling pathway (Fig. 5D, p-value < 0.05, Additional file 13: Table S5), including *TIMP1*, *ENO3*, *EGLN3*, *GAPDH*, *LDHA*, *CUL2*, *EIF4E*, and *IL6R*. These DEGs are correlated with blood pressure of the patients. *ENO3* and *IL6R* were negatively correlated with blood pressure, while *EGLN3*, *GAPDH*, and *LDHA* were positively correlated with blood pressure (Additional file 12: Fig. S5B). Therefore, we further confirmed the interaction between *FLNB-AS1* and JUNB by pulling down *FLNB-AS1* (Fig. 5E, Additional file 13: Table S6) and detecting JUNB with Western blotting (Fig. 5F). Further, we used ProbKnot to predict the secondary structure of *FLNB-AS1*, containing three pseudoknots (Frag-1: 1–1460, Frag-2: 1461–2920, Frag-3: 2921–3702) as the potential protein-binding motifs (Fig. 5G). Then, we amplified these lncRNA fragments and cloned them into expression vectors with the T7 promoter to obtain lncRNA fragments through in vitro transcription (Fig. 5H, Additional file 13: Table S7). These lncRNA fragments were subsequently biotinylated as probes to pulldown their binding proteins. The interaction between JUNB and the segments of *FLNB-AS1* was detected using silver staining and Western blotting (Fig. 5I,J). The Frag-2 showed the strongest binding affinity to JUNB (Fig. 5J).

To confirm that JUNB regulates the member of the HIF-1 signaling pathway, we detected the interactions

(See figure on next page.)

Fig. 5 The lncRNA *FLNB-AS1* interacts with JUNB to regulate the transcription of the members in HIF-1 signaling pathway. **A** *FLNB-AS1* is mainly in the nucleus using GAPDH as cytoplasm marker and U6 as nucleus marker ($n = 3$ each group, Student's *t* test). **B** The proteins interacting with *FLNB-AS1* detected by RAP-MS, including 27 TFs. **C** The number of JUNB-targeted DEGs correlated with blood pressure. **D** The enriched KEGG pathways of JUNB-targeted DEGs. **E,F** RIP assay was used to verify the *FLNB-AS1*-JUNB interaction. *FLNB-AS1* in the complex was detected using qRT-PCR (Student's *t* test) (**E**), and JUNB in the complex was detected using Western blotting (**F**). **G** The secondary structure of *FLNB-AS1* predicted by ProbKnot. **H** PCR products of the three fragments of *FLNB*-AS1 were displayed on the stained agarose gel. **I** The proteins pulled down by sense RNA of three fragments of *FLNB*-AS1 were displayed on the silvery-stained gel. **J** JUNB, pulled down by fragments of *FLNB-AS1*, was detected by Western blotting. The intensity of the bands on the blot indicates the affinity between JUNB and the fragments of *FLNB-AS1*. **K** The interactions between JUNB and the promoters of *GAPDH*, *IL6R*, *ENO3*, and *EGLN3* were detected using ChIP-qPCR ($n = 3$ per group, Student's *t* test). **L–O** The overexpression of *FLNB-AS1* (Control $n = 9$, Overexpression $n = 10$, Wilcoxon test) (**L**), the expression level of transcription factor *JUNB* (Control $n = 5$, Overexpression $n = 5$, Wilcoxon test) (**M**), the protein level of JUNB (**N**), and the expression levels of JUNB-targeted genes *GAPDH* (Control $n = 9$, Overexpression $n = 10$, Wilcoxon test), *IL6R* (Control $n = 5$, Overexpression $n = 5$, Student's *t* test), *ENO3* (Control $n = 8$, Overexpression $n = 8$, Student's *t* test), and *EGLN3* (Control $n = 9$, Overexpression $n = 10$, Wilcoxon test) (**O**) in HTR8/SVneo cells with overexpression of *FLNB-AS1*. **P** The intracellular reactive oxygen species (ROS) generation was analyzed by flow cytometry through DCFH-FA staining. Representative fluorescence images of ROS in HTR8/SVneo cells after pcDNA3.1 or pcDNA3.1-*FLNB-AS1* plasmids transfection are shown on the left, and statistical data on the right (Student's *t* test, $p = 0.0091$, $n = 3$ per group). Scale bar = 50 μM

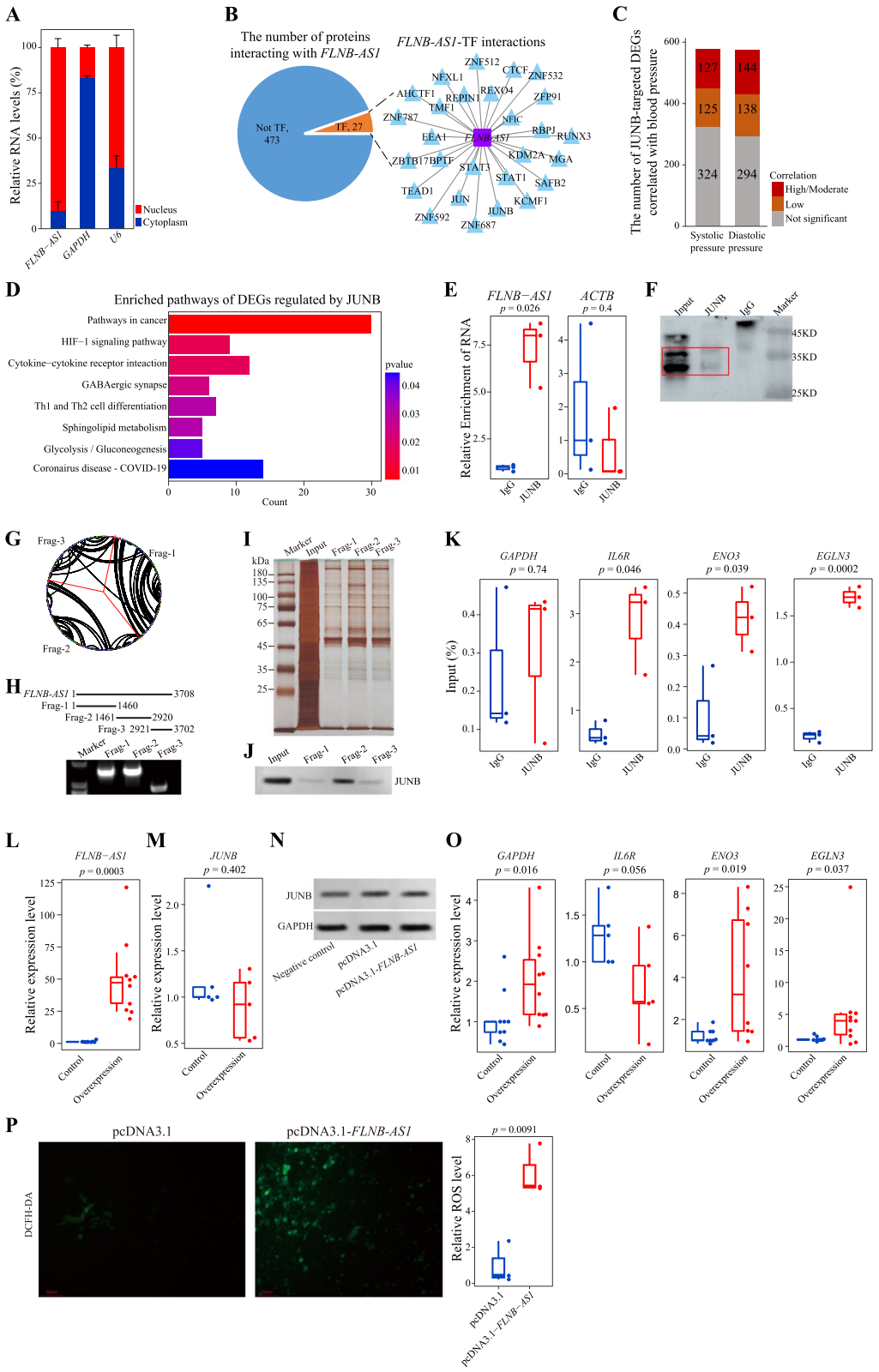

Fig. 5 (See legend on previous page.)

between JUNB and the promoters of *IL6R*, *ENO3*, *GAPDH*, and *EGLN3* using ChIP-qPCR (Fig. 5K, Additional file 13: Table S8 and Table S9). *FLNB-AS1* overexpression (Fig. 5L) did not lead to expression change of the TF JUNB in HTR8/SVneo cells (Fig. 5M,N, Additional file 13: Table S10) but significantly promoted expression of the targets *GAPDH*, *ENO3*, and *EGLN3* and inhibited the target *IL6R* (Fig. 5O). We also found that overexpression of *FLNB-AS1* induced the production of reactive oxygen species (Fig. 5P, Additional file 13: Table S11). All the results demonstrate that *FLNB-AS1* binds JUNB and regulates the transcription of genes involved in the HIF-1 signaling pathway, which may be involved in the pathogenesis of PE [59, 80].

Discussion

It is believed that the abnormal expression of genes involving placentation is the possible cause of PE [9]. We have recently carried out placental transcriptome sequencing on the placentae of PE patients classified into clinical subtypes EOSPE, LOSPE, and LOMPE and found about 3000 DEGs in EOSPE, 375 DEGs in LOSPE and 42 in LOMPE [40]. In designing our study, we had excluded confounding factors and only recruited EOSPE patients without chronic high blood pressure or kidney disease before pregnancy but with characteristics of new-onset hypertension, with significant proteinuria, and with one or more severe features such as liver function deterioration. In the current study, we revisited the transcriptome data of the placentae from EOSPE patients and normal subjects and identified 3116 DEGs, including 383 DElncRNAs. We have collected 1177 DEGs from 8 previously published papers. These DEGs only contain 2 lncRNAs, and these two lncRNAs (TCL6 and DSCR4) are overlapped with ours. Therefore, we did not consider integrating these data in the analysis of lncRNAs in regulating the differential expression.

We report our study on how the 383 DElncRNAs may cause such massive gene dysregulation in EOSPE. Several DElncRNAs reported to be associated with PE are also discovered in our study, such as *EGFR-AS1* [70], *GATA3-AS1* [81], and *MIR193BHG* [69, 82], *TCL6* [72], *SNHG12* [83], *SNHG5* [84], and *TARID* [85]. However, we miss the vital lncRNA UCA1, which has been reported to be relevant with PE recurrently [82, 86–89], because it does not meet the screening criteria for differentially expressed genes, adjusted p-value < 0.05. We constructed a high-quality DElncRNA-TF-DEG hierarchical regulatory network by integrating data from DElncRNA-TF interactions, TF-promoter bindings, and DElncRNA-promoter bindings (Fig. 3G). We performed the hierarchical clustering analysis on the regulatory network and obtained 3 clusters of DElncRNAs (Fig. 4A). Surprisingly, all 48 DElncRNAs in cluster 1 are correlated with blood pressure, respectively (Fig. 4B,C). We identified 58 KEGG pathways for the targets of the DElncRNAs in cluster 1 (Fig. 4F, Additional file 11: Table S3), including some known PE-associated pathways, such as the HIF-1 signaling pathway and ribosome pathway. In cluster 1, 62.5% (30/48) DElncRNAs are involved in the HIF-1 signaling pathway, and 29.17% (14/48) in the ribosome pathway (Fig. 4F, Additional file 11: Table S3). It has been reported that hypoxia is critical to the pathogenesis [90], and the HIF-1 signaling pathway is upregulated in PE [59, 91, 92]. The ribosome pathway is also reported to be associated with PE [65].

We ranked the lncRNAs in cluster 1 according to their importance in the hierarchical regulatory network, their association with blood pressure, and the number of targeted DEGs involved in the HIF-1 signaling pathway (Additional file 11: Table S4). The *FLNB-AS1* is in the first position. Therefore, we were particularly interested in it. The expression of *FLNB-AS1* is highly correlated with the blood pressure of the patients (Fig. 1D) and its targeted DEGs are enriched in the HIF-1 signaling pathway and ribosome pathway (Fig. 4F). Among TFs interacting with *FLNB-AS1*, JUNB is one of the fundamental TFs-driven gene expression change in EOSPE (Fig. 3A, Fig. 5B), and it is reported to have an abnormal expression in placental mesenchymal stromal cells [93]. JUNB has binding motifs in the promoters of 576 DEGs. Most interestingly, 43.75% (252/576) of the DEGs targeted by JUNB were correlated with systolic blood pressure, and 48.96% (282/576) were correlated with diastolic blood pressure (Fig. 5C). These JUNB-targeted DEGs were significantly enriched in the HIF-1 signaling pathway (Fig. 5D), a pathway known to be associated with the potential etiology of PE [59, 77]. The overexpression of *FLNB-AS1* in HTR8/SVneo cells induced expression change of JUNB-targeted genes in the HIF-1 signaling pathway, such as *GAPDH*, *ENO3*, and *EGLN3* and *IL6R* (Fig. 5O). The interactions between JUNB and the promoters of *ENO3*/*EGLN3*/*IL6R* were confirmed by ChIP-qPCR results (Fig. 5K). These results suggest that *FLNB-AS1* binds with JUNB to regulate HIF-1 signaling pathways, which is likely to be one of the most critical pathways involved in the pathogenesis of PE [59, 77].

Conclusions

The DElncRNA-TF-DEG hierarchical regulatory network contains 44.13% (169/383) DElncRNAs and 65.37% (2037/3116) DEGs in EOSPE. The DElncRNAs, which were in the top position of the hierarchical regulatory network, may lead to widespread gene expression change in the placentae of the patients, perturbing the PE

pathways such as the HIF-1 signaling pathway, and thus implicated in the pathogenesis of PE.

Limitations of study

This study provides a hierarchical lncRNA regulatory network and pathways that may be involved in the pathogenesis of EOSPE. The lncRNAs are in the top position of the hierarchical regulatory network, so they may lead to widespread gene expression change. Although we have empirically shown that 3 DElncRNAs can interact with TFs and regulate the transcription of genes, more evidence is needed to confirm the relevance of the network to PE.

Methods

Cell culture

The HTR8/SVneo cell line was obtained from the American Type Culture Collection (Manassas, USA). Cells were cultured in RPMI 1640 medium (Corning, USA) supplemented with 10% fetal bovine serum (Gibco, USA) in humidified air at 37 ℃ with 5% CO_2.

Preeclampsia patients and placental tissue collection

The project was approved by the Ethics Board of Nanfang Hospital of Southern Medical University. All patients have signed the informed consent. All samples were collected at the Department of Obstetrics & Gynecology of Nanfang Hospital in China from January 2015 to July 2016. The placenta tissue samples were mid-sections between the chorionic and maternal basal surfaces from four different placenta positions within 5 min after delivery. The tissues were washed immediately with PBS buffer and preserved in 500 μl RNAlater at − 80 ℃ for later RNA extraction. The clinical characteristics of each patient were extracted from the medical records, which strictly followed the American Board of Obstetrics and Gynecology, Williams Obstetrics 24th edition.

The diagnostic criteria for PE were as follows: new-onset hypertension (systolic blood pressure ≥ 140 mmHg and/or diastolic blood pressure ≥ 90 mmHg) on at least 2 occasions at 4 h apart 20 weeks of gestation, accompanied by one or more of the following features: proteinuria (≥ 0.3 g/24 h or more, or ≥ 2 + on dipstick analysis of urine), maternal organ dysfunction (including renal, hepatic and neurological), or hepatological involvement such as thrombocytopenia, and/ or uteroplacental dysfunction, such as fetal growth restriction. The severe PE was diagnosed if patients with PE have systolic blood pressure ≥ 160 mmHg and/or diastolic blood pressure ≥ 110 mmHg on at least 2 occasions at 4 h apart while the patients are on bed rest, accompanied by one or more of the following symptoms: significant proteinuria of ≥ 0.5 g/24 h or ≥ 3 + on dipstick analysis of urine, liver function deterioration, thrombocytopenia (platelet count < 100,000/mL), oliguria (≤ 500 mL in 24 h), creatinine ≥ 1.1 mg/dL or a doubling of the serum creatinine, cerebral or visual disturbances. According to gestational age at its diagnosis, PE can be classified into early-onset (< 34 weeks) and late-onset (≥ 34 weeks). The date of onset was defined as the gestational age when both blood pressure and proteinuria criteria were first diagnosed. All women delivered by C-section without labor were included. Exclusion criteria included pregnancies in women with a previous history of essential hypertension (chronic hypertension), type I or type II diabetes, thyroid insufficiency, cardiovascular disease, chronic inflammatory or chronic renal disease, hepatitis, and chorioamnionitis. The pregnancies with gestational hypertension and/or preterm delivery (before 37 weeks + 0 days of pregnancy) were considered as exclusion criteria for the controls. Other exclusion criteria included consecutive miscarriages (≥ 2 pregnancy losses) and/or fetal anomaly.

Based on the criteria described above, we grouped our PE patients into three clinical subtypes: (1) early-onset severe PE (EOSPE): new-onset hypertension (systolic blood pressure ≥ 160 mmHg and/or diastolic blood pressure ≥ 110 mmHg) with significant proteinuria (≥ 5 g/24 h or 3 + on urine dipstick) before 34 weeks of gestation and with one or more severe features (such as liver function deterioration, thrombocytopenia); (2) late-onset severe PE (LOPSE): similar symptoms as EOSPE, but new-onset after 34 weeks of gestation; (3) late-onset mild PE (LOMPE): new-onset hypertension accompanied proteinuria after 34 weeks of pregnancies without severe features described above. The summary of clinical characteristics of EOSPE patients and normal controls is listed in Additional file 1: Table S1.

RNA isolation and RNA-seq

According to the manufacturer's instructions, total RNA was isolated using the RNeasy Plus Universal Mini Kit (Qiagen). RNA sequencing was carried out at Berry Genomics Corporation (Beijing, China). Briefly, RNAs with polyA tails were isolated, and double-stranded cDNA libraries were prepared using the TruSeq RNA Kit (Illumina), followed by paired-end sequencing using Illumina Hiseq 2500.

qRT-PCR

RNA (500 ng) was reverse transcribed using the PrimeScriptTMRT reagent Kit (Takara, Japan), and qRT-PCR was performed with the SYBR Premix Ex TaqTM kit (Takara, Japan) in a LightCycler 480 (Roche, Swiss) system, to detect gene expression, following the manufacturer's instruction. The results were evaluated by the $2^{-\Delta\Delta CT}$ and converted to fold changes using ACTB as internal

controls (Additional file 1: Table S3-S4, Additional file 13: Table S10).

Plasmid transfection

The plasmids pcDNA3.1 and pcDNA3.1-*FLNB-AS1* were purchased from Genechem (Genechem, China). The transfection was done using Lipofectamine 3000 (Invitrogen) according to the manufacturer's instructions. After 48 h of transfection, the HTR8/SVneo cells were harvested for further experiments.

Subcellular fractionation

Following the manufacturer's instructions, cytosolic and nuclear fractions of HTR8/SVneo cells were prepared using a Nucleoprotein Extraction Kit (BestBio science, China). HTR8/SVneo cells were washed twice with ice-cold PBS and pelleted by centrifugation at 1000 *g* for 5 min. Then, 200 μl ice-cold Reagent A was added and incubated on ice for 15 min (shaken vigorously for 15 s every 5 min) and pelleted by centrifugation at 1200 *g* for 10 min at 4 ℃. The supernatants (cytoplasmic fractions) were collected for further processing. The precipitates were washed twice with PBS and pelleted by centrifugation at 2000 *g* for 5 min at 4 ℃. The deposits were the nuclear fractions. The levels of *FLNB-AS1*, *GAPDH*, and *U6* were examined by qRT-PCR (Additional file 13: Table S1). *GAPDH* was used as the cytoplasm marker, and *U6* as the nuclear marker.

RNA antisense purification with mass spectrometry (RAP-MS)

RAP-MS was performed to explore the protein partners that interact with *FLNB-AS1*. RNAstructure Webserver (RNAstructure Web Servers Manual (rochester.edu)) was used to generate the secondary structure of *FLNB-AS1*. The regions with a low probability of internal base pairings were selected for designing antisense DNA oligonucleotide probes. The probes were biotinylated at 5' ends. Ten specific probes were designed to capture *FLNB-AS1*, and two LacZ probes were used as the negative control (Additional file 13: Table S2).

Two hundred million HTR8/SVneo cells were collected for *FLNB-AS1* antisense purifications. Cells were washed twice with ice-cold PBS and UV-crosslinked on ice. Cells were collected from culture dishes and pelleted by centrifugation at 1000 *g* for 5 min. Cell Lysis was prepared as previously described [94], and nuclear lysate and whole cell lysate were prepared using 100 million HTR8/SVneo cells. Forty-microgram probes were incubated with Cell Lysis at 67 ℃ for 2 h. The probe-lysis mixture was incubated with streptavidin-coated magnetic beads (Thermo Fisher Scientific) for 2 h at room temperature on a rotator. Beads were washed 3 to 6 times, 0.5% magnetic beads were transferred to a PCR strip tube at the last wash, and the rest were stored at − 80 ℃ for mass spectrometry.

Motif-RNA-pull-down

ProbKnot was used to analyze the secondary structure of *FLNB-AS1*, which was divided into three distinct regions. Three lncRNA segments were amplified by PCR and cloned into an expression vector with a T7 promoter to obtain lncRNA fragments through in vitro transcription (Additional file 13: Table S7). These lncRNA fragments were subsequently biotinylated as probes to pull down their binding proteins. The interaction between JUNB and the segments of *FLNB-AS1* was detected using silver staining and Western blotting.

RNA immunoprecipitation assay (RIP assay)

Cellular proteins were extracted from HTR8/SVneo cells using polysome lysis buffer (100 mM KCl, 5 mM $MgCl_2$, 10 mM HEPES–NaOH, 1% NP-40) and supplemented using 1 mM DTT, 200 units/ml RiboLockRNase inhibitor, and EDTA-free Protease Inhibitor Cocktail. Protein A/G magnetic beads were used to isolate RNAs that bind with JUNB, and the same amount was used for rabbit IgG control. The amount of *FLNB-AS1* in the protein-RNA complexes was measured by qRT-PCR (Additional file 13: Table S6).

ChIP-qPCR

Cell lysates with HTR8/SVneo cells were incubated overnight with JUNB antibodies or rabbit IgG at 4 ℃ on a rotator. The immunoprecipitated DNA was quantified by qRT-PCR using primers *GAPDH*, *ENO1*, *ENO3*, and *EGLN3* to evaluate the interaction with JUNB at the target regions (Additional file 13: Table S8 and Table S9).

Intracellular ROS production assays

HTR8/SVneo cells were seeded on to 6-well plates at a density of 5×10^5 cells per well and cultured for 24 h. The cells were washed twice with PBS. Fresh medium containing 10 μM DCFH-DA were added to the wells and cells were incubated at 37 °C for 30 min. After incubation, the cells were washed three times with PBS. DCFH-DA was deacetylated intracellularly by nonspecific esterase, which was further oxidized by ROS (reactive oxygen species) to the fluorescent compound 2,7-dichlorofluorescein (DCF). DCF fluorescence intensity was determined using a fluorescence microscope. Therefore, the ROS level was represented by the DCF intensity (Additional file 13: Table S11).

Transcriptome reconstruction in tissues

Hisat [95] was used to perform reads mapping to the human genome (GRCH38) for RNA-seq data, and RSEM

[96] was used to quantify gene expression levels of GENCODE v29 (hg38) transcripts. StringTie [97] was served to reconstruct the transcriptome regarding transcripts expressed with an FPKM ≥ 0.5 in at least one sample. Each sample was applied to reconstruct the transcriptome separately. The resulting transcript models were then merged into a non-redundant set of transcripts (the uniform set for all samples, using stringtie-merge with parameters –m 300 –c 0.5 –F 0.5 –f 0.05). The expression levels of the uniform set of transcripts were quantified using RSEM. The software tximport [98] was used to merge the gene expression profile of all samples. The 16,956 genes assembled by Stingtie correspond to 16,088 gene symbols (Additional file 1: Table S5).

Computational removal of blood contamination

As the contaminated cord blood cells could not be thoroughly washed from the placenta tissue samples, the extracted RNAs contained some from cord blood cells. To better study the difference in gene expression of placenta tissues between PE patients and controls, we removed the contamination using the expression level of a cord blood marker gene for normalization. Cord blood samples from two normal pregnant women were sequenced using the same RNA-seq method. In addition, RSEM [96] was used to quantify the gene expression level in the cord blood samples (Additional file 1: Table S6). To remove the blood contamination, the Hemoglobin Subunit Mu (HBM), a subunit of hemoglobin specifically expressed in red blood cells, was used to calibrate the raw count of genes according to the following equation:

$$\mathrm{geneX}_{\mathrm{actual}} = \mathrm{geneX}_{\mathrm{placenta}} - \mathrm{geneX}_{\mathrm{cord\ blood}} \times \frac{\mathrm{HBM}_{\mathrm{placenta}}}{\mathrm{HBM}_{\mathrm{cord\ blood}}}$$

(the average of gene expression levels in cord blood samples were used in the calculation). The raw counts of genes in each sample before and after removing blood contamination are shown in Additional file 1: Table S7.

Differentially expressed gene detection

Differential expression analysis between the two groups was performed using DESeq2. Differentially expressed genes (DEGs) were determined using a cut-off of FDR < 0.05 in placentae tissues (Additional file 1: Table S2).

The correlation between the expression levels of DEGs and blood pressure

The *cor.test* function in R was used to calculate Spearman's correlation *Rho* values between the expression levels of DEGs and blood pressure. The *p*-value < 0.05 was used to determine whether the expression levels of DEGs correlate with blood pressure. For example, suppose the absolute value of *Rho* is less than 0.4, which is considered a weak correlation. In that case, the absolute value of *Rho* between 0.4 and 0.6 is considered a moderate correlation, and the absolute value of *Rho* bigger than 0.6 is considered a strong correlation (Additional file 1: Table S8).

Measure the discrimination accuracy of DElncRNAs and coding DEGs

Receiver operating characteristic (ROC) curves analysis was performed using the *roc* function in pROC (R package, v1.16.2), and the area under the curve (AUC) was used as the effective measure of accuracy (Additional file 1: Table S8).

PE candidate genes from the literature

Due to small sample sizes, the differentially expressed genes have yet to be well defined in previous microarray and transcriptomic studies. Several meta-analyses on the reported microarray have been published since 2012 [21–23, 99–101]. In 2015, the first RNA-seq study on PE was reported [102]. To obtain a consensus on PE candidate genes, we collected 1177 genes from the literature, including six meta-analysis papers [21–23, 99–101], one literature-curation paper [103], and one RNA-seq research paper [102]. These 1177 genes are PE candidate genes; their information is listed in Additional file 1: Table S9.

LncRNA-protein interaction network

RNA–protein interaction data were collected from four databases, including RNAinter [49], starBase v3.0 [47], NPInter v5.0 [50], and RNAct [48]. These DElncRNA-protein interaction data, including the curated and predicted data, are shown in Additional file 3: Table S1. To find out the transcription factors (TFs) interacting with DElncRNAs, we mapped the proteins interacting with DElncRNAs to the 1639 reliable human TFs [104].

Transcription factor and target regulation network

HOMER (Hypergeometric Optimization of Motif EnRichment) [105] was used to search for the transcription factor binding sites (TFBS) in promoter regions of DEGs (from 1.5 kb upstream to 0.5 kb downstream of transcription start sites) in EOSPE. The matches between TFs and TFBSs were manually checked. TFs without expression in the placenta transcriptome were removed. The TFs with significantly enriched TFBS and their corresponding target genes were used to construct the TF-target regulatory network (Additional file 5: Table S1 and Table S2).

LncRNA-DNA triplex structure prediction

The TDF (Triplex Domain Finder) [68] was used to predict the triplex helix formation between 383 DElncRNAs and the promoter regions (upstream 2000 bp from TSSs) of 3116 DEGs (Additional file 7: Table S1). Each triplex is formed by one RNA sequence (triplex-forming oligo, TFO) and a DNA region (triplex target sites, TTS).

Co-expression network construction

The *rcorr* function in Hmisc (R package, v4.4) was used to calculate the Pearson correlation among all expressed genes in placentae based on the TPM (transcript per million) value. The FDR < 0.05 was set as the cutoff to extract the significant correlation between DElncRNAs and the other DEGs in EOSPE (Additional file 8: Table S1).

LncRNA-TF-DEG hierarchical regulatory network construction

The lncRNA-TF-DEG hierarchical regulatory network was constructed by integrating curated lncRNA-TF interactions and TF-target regulatory, then filtering with DElncRNA-promoter interactions and DElncRNA-DEG co-expression (Additional file 10: Table S1). For each DElncRNA in the DElncRNA-TF-DEG network, the enrichment of lncRNA-targeted DEGs (whose promoters interact with the lncRNA and the expression levels are also significantly correlated with the lncRNA) in the TF-targeted DEGs (whose promoters harbor the binding sites of the TFs) was calculated, and the DElncRNA with p-value < 0.05 was considered to be more likely to regulate gene expression by serving as a scaffold between TF and promoter regions (Additional file 10: Table S2). The DElncRNA with a significant enrichment score (p-value < 0.05) was kept to construct a high-quality core DElncRNA-TF-DEG hierarchical regulatory network.

Hierarchical clustering analysis for DElncRNAs

The hierarchical clustering analysis for DElncRNAs was performed based on the shared targets and the correlation with blood pressure. The Jaccard index between DElncRNAs was calculated by *jaccardSets* function in R. If the paired DElncRNAs are significantly correlated with blood pressure, the Jaccard index is multiplied by 8; if one of the paired DElncRNAs is significantly correlated with blood pressure, the Jaccard index is multiplied by 4; if none of the paired DElncRNAs is significantly correlated with blood pressure, the Jaccard index is multiplied by 1. The final matrix was used to do the hierarchical clustering analysis (Additional file 11: Table S1 and Table S2).

Mass spectrometry data analysis

Mass spectrometry was carried out at Wininnovate Biology Corporation (Shenzhen, China). The MS/MS data were analyzed for protein identification and quantification using PEAKS Studio 8.5. The local false discovery rate at PSM was 1.0% after searching against Homo sapiens database with a maximum of two missed cleavages. The following settings were selected: Oxidation (M), Acetylation (Protein N-term), Deamidation (NQ), Pyro-glu from E, and Pyro-glu from Q for variable modifications as well as fixed Carbamidomethylation of cysteine. Precursor and fragment mass tolerance was set to 10 ppm and 0.05 Da, respectively. Compared with the LacZ pulldown complexes, proteins only in the *FLNB-AS1* pulldown complexes are considered to interact with *FLNB-AS1* (Additional file 13: Table S3 and Table S4).

KEGG pathway enrichment analysis

KEGG (Kyoto Encyclopedia of Genes and Genomes) pathway enrichment analysis was performed with the clusterProfiler package [106]. A cutoff of p-value < 0.05 and q-value < 0.2 were used to determine the enriched pathways of DEGs regulated by DElncRNAs in the core hierarchical regulatory network. A cutoff of p-value < 0.05 was used to determine the enriched pathways of DEGs regulated by JUNB.

GO terms enrichment analysis

Gene Ontology terms (Biological Process, Cellular Component, Molecular Function) enrichment analyses were also using the clusterProfiler package [106], and the adjusted p-value < 0.05 was set as a cutoff to select the enriched terms. The semantic similarity-based method (RRVGO, R package, https://ssayols.github.io/rrvgo) was used to summarize the enriched GO terms.

Statistical analysis

All enrichment analyses were performed on the R platform, and one-tailed Fisher's exact test was used. Error bars represent the standard deviation of the fraction, estimated with a bootstrapping method with 100 resamplings. The function of *shapiro.test* in R was used to detect the normality of the data. The current study used the Wilcoxon rank-sum test or Student's t test to identify differences between two groups according to the data type. Statistical significance was described as * $p < 0.05$, ** $p < 0.01$ and *** $p < 0.001$.

Abbreviations

PE	Preeclampsia
EOSPE	Early-onset severe preeclampsia
LOSPE	Late-onset severe preeclampsia
LOMPE	Late-onset mild preeclampsia
DEG	Differentially expressed genes
lncRNA	Long non-coding RNA
DElncRNA	Differentially expressed lncRNA
RAP-MS	RNA antisense purification followed by mass spectrometry
RIP	RNA immunoprecipitation
ROC	Receiver operating characteristic
AUC	Area under the curve
ROS	Reactive oxygen species

Supplementary Information

The online version contains supplementary material available at https://doi.org/10.1186/s12915-024-01959-1.

Additional file 1: Table S1. Clinical information for transcriptome sequencing samples. Table S2. Total DEGs in EOSPE were identified using DESeq2. Table S3. The qRT-PCR primer sequences for detecting genes. Table S4. The qRT-PCR results of detecting genes in placentae. Table S5. The raw counts of genes in the placenta before removing the cord blood contamination. Table S6. The raw counts of genes in cord blood samples. Table S7. The raw counts of genes in the placenta after removing the cord blood contamination. Table S8. The correlation between blood pressure and DElncRNA/coding DEGs, and the discrimination accuracy of DElncRNAs and coding DEGs. Table S9. Known PE-associated genes are collected from the literature.

Additional file 2: Figure S1. Differentially-expressed genes in placentae of patients with EOSPE.

Additional file 3: Table S1. DElncRNA-protein interaction data were collected from databases, including curated and predicted data. Table S2. The enriched KEGG pathways of all proteins interacting with DElncRNAs in EOSPE. Table S3. The enriched GO terms of all proteins interacting with DElncRNAs in EOSPE. Table S4. The enriched KEGG pathways of DEG-encoded proteins interacting with DElncRNAs. Table S5. The enriched GO MF terms of DEG-encoded proteins interacting with DElncRNAs. Table S6. The enriched KEGG pathways of all DEGs in EOSPE. Table S7. The statistic table for each DElncRNA in the DElncRNA-protein interaction network. For each DElncRNA, the enrichment score is calculated to determine whether its interacting proteins are enriched with TFs. The enrichment scoreis calculated using a One-sided Fisher's exact test.

Additional file 4: Figure S2. The enriched pathways and molecular functions of proteins interacting with DElncRNA.

Additional file 5: Table S1. TF-target regulatory network predicted by HOMER. Table S2. Significant transcription factor binding sites in the promoter of DEGs and their corresponding transcription factors.

Additional file 6: Figure S3. The predicted TFs and their targeted DEGs.

Additional file 7: Table S1. DElncRNAs form triplex structures with promoters of DEGs.

Additional file 8: Table S1. The DElncRNA-DEG co-expression network.

Additional file 9: Figure S4. Construction of DElncRNA-TF-DEG hierarchical regulatory network.

Additional file 10: Table S1. The DElncRNA-TF-DEG hierarchical regulatory network. The hierarchical regulatory network includes 3 types of interaction: DElncRNA-TF interaction, lncRNA and promoter of DEGs in EOSPE interaction, and TF-DEG regulatory interaction. Table S2. The statistic table of DElncRNA in DElncRNA-TF-DEG hierarchical regulatory network. The table includes the number of interacting TFs, the number of DEGs regulated by interacting TFs, the number of DEGs in the DElncRNA-TF-DEG hierarchical regulatory network, the number of DEGs forming triplex with DElncRNA, and the log2 FoldChange of DElncRNA. The *p*-value was calculated using a One-sided Fisher's exact test. DElncRNAs are more likely to serve as a scaffold for TF-promoter interactions if the *p*-value is less than 0.05. Table S3. The enriched KEGG pathways of DEGs in the DElncRNA-TF-DEG hierarchical regulatory network.

Additional file 11: Table S1. The matrix shows the target similarity of DElncRNAs. Table S2. The cluster information of DElncRNAs. Table S3. The enriched KEGG pathways of DEGs regulated by each DElncRNA in cluster 1. Table S4. The statistic table of 30 DElncRNA in C1, in which their targeted DEGs are significantly enriched with the HIF-1 signaling pathway. According to their importance in the hierarchical networkand their association with blood pressureand the number of targeted DEGs involved in HIF-1signaling pathway, we calculated the mean rank to sort these 30 DElncRNAs by ascending way.

Additional file 12: Figure S5. The DElncRNAs in cluster 2 and the DEGs are involved in the HIF-1 signaling pathway, galactose metabolism, and the ribosome.

Additional file 13: Table S1. The subcellular location of *FLNB-AS1*. Table S2. The probe sequences for the RAP experiments. Table S3. The proteins interacting with *FLNB-AS1*. Table S4. The mass spectrometry result. Table S5. The enriched KEGG pathways of DEGs regulated by JUNB. Table S6. The immunoprecipitation of Protein RNA Complexes. Table S7. The primers used to obtain *FLNB-AS1*'s 3 protein binding motifs. Table S8. The ChIP-qPCR primer sequences of the promoters. Table S9. The ChIP-qPCR results of detecting genes in HTR8/SVneo cells. Table S10. The qRT-PCR results of detecting genes in HTR8/SVneo cells. Table S11. The intracellular ROS production assay results induced by overexpression *FLNB-AS1* in HTR8/SVneo cells.

Additional file 14: Uncropped gels and blots.

Acknowledgements
We thank the patients for their generous support for this study.

Authors' contributions
XPY conceived the project; HHL analyzed the data; JL, XLW, QC2, CQX, MZ, and CLC recruited the patients and normal subjects, collected and analyzed the clinical information; QC1, SJJ, YLC, and JW collected the tissue samples. YJL, QC1, and SSJ performed the experimental validation; ZJW and YG participated in data analysis, and HHL and XPY wrote the paper. All authors read and approved the final manuscript.

Funding
This work was supported by National Natural Science Foundation of China grants No. 31771434 (X.Y.) and No. 81671466 (M.Z.), the Natural Science Foundation of Guangdong Province grant No. 2016A030308020 (X.Y.), Basic and Applied Basic Research Foundation of Guangdong Province grant No. 2019B1515120080 (X.Y.), and the Science and Technology Planning Project of Guangdong Province grant No. 2017B020227010 (X.Y.). The President Foundation of Nanfang Hospital, Southern Medical University, grant No. 2020B009 (H.L.).

Availability of data and materials
All data generated or analyzed during this study are included in this published article and its supplementary information files. The RNA-seq raw data are available at GEO (accession number GSE148241), which have been published by our previous work [40, 107].

Declarations

Ethics approval and consent to participate
This research has been approved by the Ethics Board of Nanfang Hospital of Southern Medical University (Reference NFEC-201601-K1), and all patients have signed the informed consent.

Consent for publication
Not applicable.

Competing interests
The authors declare that they have no competing interests.

Received: 12 April 2023 Accepted: 15 July 2024
Published online: 29 July 2024

References

1. Duley L. The global impact of pre-eclampsia and eclampsia. Semin Perinatol. 2009;33(3):130–7.

2. Abalos E, Cuesta C, Grosso AL, Chou D, Say L. Global and regional estimates of preeclampsia and eclampsia: a systematic review. Eur J Obstet Gynecol Reprod Biol. 2013;170(1):1–7.
3. Logue OC, George EM, Bidwell GL 3rd. Preeclampsia and the brain: neural control of cardiovascular changes during pregnancy and neurological outcomes of preeclampsia. Clin Sci. 2016;130(16):1417–34.
4. Eneroth-Grimfors E, Westgren M, Ericson M, Ihrman-Sandahl C, Lindblad LE. Autonomic cardiovascular control in normal and pre-eclamptic pregnancy. Acta Obstet Gynecol Scand. 1994;73(9):680–4.
5. Melchiorre K, Sharma R, Thilaganathan B. Cardiovascular implications in preeclampsia: an overview. Circulation. 2014;130(8):703–14.
6. Voss A, Baumert M, Baier V, Stepan H, Walther T, Faber R. Autonomic cardiovascular control in pregnancies with abnormal uterine perfusion. Am J Hypertens. 2006;19(3):306–12.
7. WHO Guidelines Approved by the Guidelines Review Committee. In: WHO Recommendations for Prevention and Treatment of Pre-Eclampsia and Eclampsia. Geneva: World Health Organization Copyright © 2011, World Health Organization; 2011.
8. Zeeman GG. Neurologic complications of pre-eclampsia. Semin Perinatol. 2009;33(3):166–72.
9. Mol BWJ, Roberts CT, Thangaratinam S, Magee LA, de Groot CJM, Hofmeyr GJ. Pre-eclampsia. Lancet. 2016;387(10022):999–1011.
10. Davies EL, Bell JS, Bhattacharya S. Preeclampsia and preterm delivery: A population-based case-control study. Hypertens Pregnancy. 2016;35(4):510–9.
11. Mitani M, Matsuda Y, Makino Y, Akizawa Y, Ohta H. Clinical features of fetal growth restriction complicated later by preeclampsia. J Obstet Gynaecol Res. 2009;35(5):882–7.
12. Weiler J, Tong S, Palmer KR. Is fetal growth restriction associated with a more severe maternal phenotype in the setting of early onset preeclampsia? A retrospective study. PLoS ONE. 2011;6(10):e26937.
13. Liu X, Zhao W, Liu H, Kang Y, Ye C, Gu W, Hu R, Li X. Developmental and Functional Brain Impairment in Offspring from Preeclampsia-Like Rats. Mol Neurobiol. 2016;53(2):1009–19.
14. Griffith MI, Mann JR, McDermott S. The risk of intellectual disability in children born to mothers with preeclampsia or eclampsia with partial mediation by low birth weight. Hypertens Pregnancy. 2011;30(1):108–15.
15. Wu CS, Sun Y, Vestergaard M, Christensen J, Ness RB, Haggerty CL, Olsen J. Preeclampsia and risk for epilepsy in offspring. Pediatrics. 2008;122(5):1072–8.
16. Trosse C, Ravneberg H, Stern B, Pryme IF. Vectors encoding seven oikosin signal peptides transfected into CHO cells differ greatly in mediating Gaussia luciferase and human endostatin production although mRNA levels are largely unaffected. Gene regulation and systems biology. 2007;1:303–12.
17. Walker CK, Krakowiak P, Baker A, Hansen RL, Ozonoff S, Hertz-Picciotto I. Preeclampsia, placental insufficiency, and autism spectrum disorder or developmental delay. JAMA Pediatr. 2015;169(2):154–62.
18. Dachew BA, Mamun A, Maravilla JC, Alati R. Pre-eclampsia and the risk of autism-spectrum disorder in offspring: meta-analysis. The British journal of psychiatry : the journal of mental science. 2018;212(3):142–7.
19. Dalman C, Allebeck P, Cullberg J, Grunewald C, Koster M. Obstetric complications and the risk of schizophrenia: a longitudinal study of a national birth cohort. Arch Gen Psychiatry. 1999;56(3):234–40.
20. Ursini G, Punzi G, Chen Q, Marenco S, Robinson JF, Porcelli A, Hamilton EG, Mitjans M, Maddalena G, Begemann M, et al. Convergence of placenta biology and genetic risk for schizophrenia. Nat Med. 2018;24(6):792–801.
21. Moslehi R, Mills JL, Signore C, Kumar A, Ambroggio X, Dzutsev A. Integrative transcriptome analysis reveals dysregulation of canonical cancer molecular pathways in placenta leading to preeclampsia. Sci Rep. 2013;3:2407.
22. Vaiman D, Miralles F. An Integrative Analysis of Preeclampsia Based on the Construction of an Extended Composite Network Featuring Protein-Protein Physical Interactions and Transcriptional Relationships. PLoS ONE. 2016;11(11):e0165849.
23. Tejera E, Cruz-Monteagudo M, Burgos G, Sanchez ME, Sanchez-Rodriguez A, Perez-Castillo Y, Borges F, Cordeiro M, Paz YMC, Rebelo I. Consensus strategy in genes prioritization and combined bioinformatics analysis for preeclampsia pathogenesis. BMC Med Genomics. 2017;10(1):50.
24. Ulitsky I, Bartel DP. lincRNAs: genomics, evolution, and mechanisms. Cell. 2013;154(1):26–46.
25. Iyer MK, Niknafs YS, Malik R, Singhal U, Sahu A, Hosono Y, Barrette TR, Prensner JR, Evans JR, Zhao S, et al. The landscape of long noncoding RNAs in the human transcriptome. Nat Genet. 2015;47(3):199–208.
26. Zhang Y, Pitchiaya S, Cieslik M, Niknafs YS, Tien JC, Hosono Y, Iyer MK, Yazdani S, Subramaniam S, Shukla SK, et al. Analysis of the androgen receptor-regulated lncRNA landscape identifies a role for ARLNC1 in prostate cancer progression. Nat Genet. 2018;50(6):814–24.
27. Delas MJ, Jackson BT, Kovacevic T, Vangelisti S, Munera Maravilla E, Wild SA, Stork EM, Erard N, Knott SRV, Hannon GJ. lncRNA Spehd Regulates Hematopoietic Stem and Progenitor Cells and Is Required for Multilineage Differentiation. Cell Rep. 2019;27(3):719–729 e716.
28. Quek XC, Thomson DW, Maag JL, Bartonicek N, Signal B, Clark MB, Gloss BS, Dinger ME. lncRNAdb v2.0: expanding the reference database for functional long noncoding RNAs. Nucleic Acids Res. 2015;43(Database issue):D168–173.
29. Wang Y, Wang Z, Xu J, Li J, Li S, Zhang M, Yang D. Systematic identification of non-coding pharmacogenomic landscape in cancer. Nat Commun. 2018;9(1):3192.
30. Ma L, Cao J, Liu L, Du Q, Li Z, Zou D, Bajic VB, Zhang Z. LncBook: a curated knowledgebase of human long non-coding RNAs. Nucleic Acids Res. 2019;47(D1):D128–34.
31. Statello L, Guo CJ, Chen LL, Huarte M. Gene regulation by long non-coding RNAs and its biological functions. Nat Rev Mol Cell Biol. 2021;22(2):96–118.
32. Zhou L, Sun K, Zhao Y, Zhang S, Wang X, Li Y, Lu L, Chen X, Chen F, Bao X, et al. Linc-YY1 promotes myogenic differentiation and muscle regeneration through an interaction with the transcription factor YY1. Nat Commun. 2015;6:10026.
33. Mondal T, Subhash S, Vaid R, Enroth S, Uday S, Reinius B, Mitra S, Mohammed A, James AR, Hoberg E, et al. MEG3 long noncoding RNA regulates the TGF-beta pathway genes through formation of RNA-DNA triplex structures. Nat Commun. 2015;6:7743.
34. Zhang X, Jiang Q, Li J, Zhang S, Cao Y, Xia X, Cai D, Tan J, Chen J, Han JJ. KCNQ1OT1 promotes genome-wide transposon repression by guiding RNA-DNA triplexes and HP1 binding. Nat Cell Biol. 2022;24(11):1617–29.
35. Mohammadpour-Gharehbagh A, Jahantigh D, Saravani M, Harati-Sadegh M, Maruie-Milan R, Teimoori B, et al. Impact of HOTAIR variants on preeclampsia susceptibility based on blood and placenta and in silico analysis. IUBMB Life. 2019;71(9):1367–81.
36. Zhang Y, Zou Y, Wang W, Zuo Q, Jiang Z, Sun M, De W, Sun L. Downregulated long non-coding RNA MEG3 and its effect on promoting apoptosis and suppressing migration of trophoblast cells. J Cell Biochem. 2015;116(4):542–50.
37. Zuo Q, Huang S, Zou Y, Xu Y, Jiang Z, Zou S, Xu H, Sun L. The Lnc RNA SPRY4-IT1 Modulates Trophoblast Cell Invasion and Migration by Affecting the Epithelial-Mesenchymal Transition. Sci Rep. 2016;6:37183.
38. Xu Y, Ge Z, Zhang E, Zuo Q, Huang S, Yang N, Wu D, Zhang Y, Chen Y, Xu H, et al. The lncRNA TUG1 modulates proliferation in trophoblast cells via epigenetic suppression of RND3. Cell Death Dis. 2017;8(10):e3104.
39. Chen H, Meng T, Liu X, Sun M, Tong C, Liu J, Wang H, Du J. Long non-coding RNA MALAT-1 is downregulated in preeclampsia and regulates proliferation, apoptosis, migration and invasion of JEG-3 trophoblast cells. Int J Clin Exp Pathol. 2015;8(10):12718–27.
40. Ren Z, Gao Y, Gao Y, Liang G, Chen Q, Jiang S, Yang X, Fan C, Wang H, Wang J, et al. Distinct placental molecular processes associated with early-onset and late-onset preeclampsia. Theranostics. 2021;11(10):5028–44.
41. Chen Q, Jiang S, Liu H, Gao Y, Yang X, Ren Z, Gao Y, Xiao L, Hu H, Yu Y, et al. Association of lncRNA SH3PXD2A-AS1 with preeclampsia and its function in invasion and migration of placental trophoblast cells. Cell Death Dis. 2020;11(7):583.
42. Jiang S, Chen Q, Liu H, Gao Y, Yang X, Ren Z, Gao Y, Xiao L, Zhong M, Yu Y, et al. Preeclampsia-Associated lncRNA INHBA-AS1 Regulates the Proliferation, Invasion, and Migration of Placental Trophoblast Cells. Mol Ther Nucleic Acids. 2020;22:684–95.
43. Gillmore T, Farrell A, Alahari S, Sallais J, Kurt M, Park C, Ausman J, Litvack M, Post M, Caniggia I. Dichotomy in hypoxia-induced mitochondrial fission in placental mesenchymal cells during development and

preeclampsia: consequences for trophoblast mitochondrial homeostasis. Cell Death Dis. 2022;13(2):191.
44. Li X, Yang N, Wu Y, Wang X, Sun J, Liu L, Zhang F, Gong Y, Zhang Y, Li X, et al. Hypoxia regulates fibrosis-related genes via histone lactylation in the placentas of patients with preeclampsia. J Hypertens. 2022;40(6):1189–98.
45. Nagano T, Mitchell JA, Sanz LA, Pauler FM, Ferguson-Smith AC, Feil R, Fraser P. The Air noncoding RNA epigenetically silences transcription by targeting G9a to chromatin. Science. 2008;322(5908):1717–20.
46. Khalil AM, Rinn JL. RNA-protein interactions in human health and disease. Semin Cell Dev Biol. 2011;22(4):359–65.
47. Li JH, Liu S, Zhou H, Qu LH, Yang JH. starBase v2.0: decoding miRNA-ceRNA, miRNA-ncRNA and protein-RNA interaction networks from large-scale CLIP-Seq data. Nucleic acids research. 2014;42(Database issue):D92–97.
48. Lang B, Armaos A, Tartaglia GG. RNAct: Protein-RNA interaction predictions for model organisms with supporting experimental data. Nucleic Acids Res. 2019;47(D1):D601–6.
49. Lin Y, Liu T, Cui T, Wang Z, Zhang Y, Tan P, Huang Y, Yu J, Wang D. RNAInter in 2020: RNA interactome repository with increased coverage and annotation. Nucleic Acids Res. 2020;48(D1):D189–97.
50. Zheng Y, Luo H, Teng X, Hao X, Yan X, Tang Y, Zhang W, Wang Y, Zhang P, Li Y, et al. NPInter v5.0: ncRNA interaction database in a new era. Nucleic Acids Res. 2023;51(D1):D232–9.
51. Li Q, Zhang J, Su DM, Guan LN, Mu WH, Yu M, Ma X, Yang RJ. lncRNA TUG1 modulates proliferation, apoptosis, invasion, and angiogenesis via targeting miR-29b in trophoblast cells. Hum Genomics. 2019;13(1):50.
52. Wu HY, Wang XH, Liu K, Zhang JL. LncRNA MALAT1 regulates trophoblast cells migration and invasion via miR-206/IGF-1 axis. Cell Cycle. 2020;19(1):39–52.
53. Xu Y, Wu D, Liu J, Huang S, Zuo Q, Xia X, Jiang Y, Wang S, Chen Y, Wang T, et al. Downregulated lncRNA HOXA11-AS Affects Trophoblast Cell Proliferation and Migration by Regulating RND3 and HOXA7 Expression in PE. Mol Ther Nucleic Acids. 2018;12:195–206.
54. Xufei F, Xiujuan Z, Jianyi L, Liyan Y, Ting Y, Min H. Up-regulation of LncRNA NEAT1 induces apoptosis of human placental trophoblasts. Free Radical Res. 2020;54(8–9):678–86.
55. Yu Z, Zhang Y, Zheng H, Gao Q, Wang H. LncRNA SNHG16 regulates trophoblast functions by the miR-218-5p/LASP1 axis. J Mol Histol. 2021;52(5):1021–33.
56. Zhang T, Bian Q, Chen Y, Wang X, Yu S, Liu S, Ji P, Li L, Shrestha M, Dong S, et al. Dissecting human trophoblast cell transcriptional heterogeneity in preeclampsia using single-cell RNA sequencing. Mol Genet Genomic Med. 2021;9(8):e1730.
57. Xu YH, Liu K, Yan J, Wang HP, Wu HY. Function and mechanism of histone demethytransferase Jmjd3 mediated regulation of Th1/Th2 balance through epigenetic modification in pre-eclampsia. Zhonghua Bing Li Xue Za Zhi. 2020;49(10):1041–5.
58. Gao X, Wang J, Shi J, Sun Q, Jia N, Li H. The Efficacy Mechanism of Epigallocatechin Gallate against Pre-Eclampsia based on Network Pharmacology and Molecular Docking. Reprod Sci. 2022;29(6):1859–73.
59. Iriyama T, Wang W, Parchim NF, Song A, Blackwell SC, Sibai BM, Kellems RE, Xia Y. Hypoxia-independent upregulation of placental hypoxia inducible factor-1alpha gene expression contributes to the pathogenesis of preeclampsia. Hypertension. 2015;65(6):1307–15.
60. Rajakumar A, Brandon HM, Daftary A, Ness R, Conrad KP. Evidence for the functional activity of hypoxia-inducible transcription factors overexpressed in preeclamptic placentae. Placenta. 2004;25(10):763–9.
61. Zhang J, Huang J, Zhao Y, Zhang W. The preventive effects of aspirin on preeclampsia based on network pharmacology and bioinformatics. J Hum Hypertens. 2022;36(8):753–9.
62. Liu J, Song G, Meng T, Zhao G. Identification of Differentially Expressed Genes and Signaling Pathways in Placenta Tissue of Early-Onset and Late-Onset Pre-Eclamptic Pregnancies by Integrated Bioinformatics Analysis. Med Sci Monit. 2020;26:e921997.
63. Liu JJ, Zhang L, Zhang FF, Luan T, Yin ZM, Rui C, Ding HJ. Influence of miR-34a on preeclampsia through the Notch signaling pathway. Eur Rev Med Pharmacol Sci. 2019;23(3):923–31.
64. Gong F, Chai W, Wang J, Cheng H, Shi Y, Cui L, Jia G. miR-214-5p suppresses the proliferation, migration and invasion of trophoblast cells in pre-eclampsia by targeting jagged 1 to inhibit notch signaling pathway. Acta Histochem. 2020;122(3):151527.
65. Chen X, Tong C, Li H, Peng W, Li R, Luo X, Ge H, Ran Y, Li Q, Liu Y, et al. Dysregulated Expression of RPS4Y1 (Ribosomal Protein S4, Y-Linked 1) Impairs STAT3 (Signal Transducer and Activator of Transcription 3) Signaling to Suppress Trophoblast Cell Migration and Invasion in Preeclampsia. Hypertension. 2018;71(3):481–90.
66. Postepska-Igielska A, Giwojna A, Gasri-Plotnitsky L, Schmitt N, Dold A, Ginsberg D, Grummt I. LncRNA Khps1 Regulates Expression of the Proto-oncogene SPHK1 via Triplex-Mediated Changes in Chromatin Structure. Mol Cell. 2015;60(4):626–36.
67. Li X, Guo G, Lu M, Chai W, Li Y, Tong X, et al. Long noncoding RNA Lnc-MxA inhibits beta interferon transcription by forming RNA-DNA triplexes at its promoter. J Virol. 2019;93(21):e00786–19.
68. Kuo CC, Hanzelmann S, Senturk Cetin N, Frank S, Zajzon B, Derks JP, Akhade VS, Ahuja G, Kanduri C, Grummt I, et al. Detection of RNA-DNA binding sites in long noncoding RNAs. Nucleic Acids Res. 2019;47(6):e32.
69. Dong N, Li D, Cai H, Shi L, Huang L. Expression of lncRNA MIR193BHG in serum of preeclampsia patients and its clinical significance. J Gynecol Obstet Hum Reprod. 2022;51(5):102357.
70. Zhao ZM, Jiang J. Lowly expressed EGFR-AS1 promotes the progression of preeclampsia by inhibiting the EGFR-JAK/STAT signaling pathway. Eur Rev Med Pharmacol Sci. 2018;22(19):6190–7.
71. Zhang Z, Wang P, Zhang L, Huang C, Gao J, Li Y, Yang B. Identification of Key Genes and Long Noncoding RNA-Associated Competing Endogenous RNA (ceRNA) Networks in Early-Onset Preeclampsia. Biomed Res Int. 2020;2020:1673486.
72. Wu JL, Wang YG, Gao GM, Feng L, Guo N, Zhang CX. Overexpression of lncRNA TCL6 promotes preeclampsia progression by regulating PTEN. Eur Rev Med Pharmacol Sci. 2019;23(10):4066–72.
73. Li R, Wang N, Xue M, Long W, Cheng C, Mi C, Gao Z. A potential regulatory network among WDR86-AS1, miR-10b-3p, and LITAF is possibly involved in preeclampsia pathogenesis. Cell Signal. 2019;55:40–52.
74. Xue L, Xie K, Wu L, Yu X, Long W, Li C, Jia R, Ding H. A novel peptide relieves endothelial cell dysfunction in preeclampsia by regulating the PI3K/mTOR/HIF1alpha pathway. Int J Mol Med. 2021;47(1):276–88.
75. Mayrink J, Leite DF, Nobrega GM, Costa ML, Cecatti JG. Prediction of pregnancy-related hypertensive disorders using metabolomics: a systematic review. BMJ Open. 2022;12(4):e054697.
76. Christiane Y, Aghayan M, Emonard H, Lallemand A, Mahieu P, Foidart JM. Galactose alpha 1–3 galactose and anti-alpha galactose antibody in normal and pathological pregnancies. Placenta. 1992;13(5):475–87.
77. Nikuei P, Rajaei M, Roozbeh N, Mohseni F, Poordarvishi F, Azad M, Haidari S. Diagnostic accuracy of sFlt1/PlGF ratio as a marker for preeclampsia. BMC Pregnancy Childbirth. 2020;20(1):80.
78. Zeisler H, Llurba E, Chantraine F, Vatish M, Staff AC, Sennstrom M, Olovsson M, Brennecke SP, Stepan H, Allegranza D, et al. Predictive Value of the sFlt-1:PlGF Ratio in Women with Suspected Preeclampsia. N Engl J Med. 2016;374(1):13–22.
79. Lv H, Tong J, Yang J, Lv S, Li WP, Zhang C, Chen ZJ. Dysregulated Pseudogene HK2P1 May Contribute to Preeclampsia as a Competing Endogenous RNA for Hexokinase 2 by Impairing Decidualization. Hypertension. 2018;71(4):648–58.
80. Tal R, Shaish A, Barshack I, Polak-Charcon S, Afek A, Volkov A, Feldman B, Avivi C, Harats D. Effects of hypoxia-inducible factor-1alpha overexpression in pregnant mice: possible implications for preeclampsia and intrauterine growth restriction. Am J Pathol. 2010;177(6):2950–62.
81. Zhang Y, Liu H, Shu X, Sun Y, Chen X. Overexpressed lncRNA GATA3-AS1 in Preeclampsia and Its Effects on Trophoblast Proliferation and Migration by the miR-488-3p/ROCK1 Axis. Crit Rev Eukaryot Gene Expr. 2022;32(5):33–45.
82. Apicella C, Ruano CSM, Jacques S, Gascoin G, Mehats C, Vaiman D, Miralles F. Urothelial Cancer Associated 1 (UCA1) and miR-193 Are Two Non-coding RNAs Involved in Trophoblast Fusion and Placental Diseases. Front Cell Dev Biol. 2021;9:633937.
83. Zhou F, Sun Y, Chi Z, Gao Q, Wang H. Long noncoding RNA SNHG12 promotes the proliferation, migration, and invasion of trophoblast cells by regulating the epithelial-mesenchymal transition and cell cycle. J Int Med Res. 2020;48(6):300060520922339.

84. Yang Y, Xi L, Ma Y, Zhu X, Chen R, Luan L, Yan J, An R. The lncRNA small nucleolar RNA host gene 5 regulates trophoblast cell proliferation, invasion, and migration via modulating miR-26a-5p/N-cadherin axis. J Cell Biochem. 2019;120(3):3173–84.
85. Liao L, Liu M, Gao Y, Wei X, Yin Y, Gao L, Zhou R. The long noncoding RNA TARID regulates the CXCL3/ERK/MAPK pathway in trophoblasts and is associated with preeclampsia. Reprod Biol Endocrinol. 2022;20(1):159.
86. Wu S, Cui Y, Zhao H, Xiao X, Gong L, Xu H, Zhou Q, Ma D, Li X. Trophoblast Exosomal UCA1 Induces Endothelial Injury through the PFN1-RhoA/ROCK Pathway in Preeclampsia: A Human-Specific Adaptive Pathogenic Mechanism. Oxid Med Cell Longev. 2022;2022:2198923.
87. Penailillo R, Monteiro LJ, Acuna-Gallardo S, Garcia F, Velasquez V, Correa P, et al. Identification of LOC101927355 as a novel biomarker for preeclampsia. Biomedicines. 2022;10(6):1253.
88. Liu J, Luo C, Zhang C, Cai Q, Lin J, Zhu T, Huang X. Upregulated lncRNA UCA1 inhibits trophoblast cell invasion and proliferation by downregulating JAK2. J Cell Physiol. 2020;235(10):7410–9.
89. Ding Y, Yuan X, Gu W, Lu L. Treatment with metformin prevents preeclampsia by suppressing migration of trophoblast cells via modulating the signaling pathway of UCA1/miR-204/MMP-9. Biochem Biophys Res Commun. 2019;520(1):115–21.
90. Rana S, Lemoine E, Granger JP, Karumanchi SA. Preeclampsia: Pathophysiology, Challenges, and Perspectives. Circ Res. 2019;124(7):1094–112.
91. Kapustin RV, Kopteeva EV, Alekseenkova EN, Tral TG, Tolibova GK, Arzhanova ON. Placental expression of endoglin, placental growth factor, leptin, and hypoxia-inducible factor-1 in diabetic pregnancy and pre-eclampsia. Gynecol Endocrinol. 2021;37(sup1):35–9.
92. Jin M, Xu S, Cao B, Xu Q, Yan Z, Ren Q, Lin C, Tang C. Regulator of G protein signaling 2 is inhibited by hypoxia-inducible factor-1alpha/E1A binding protein P300 complex upon hypoxia in human preeclampsia. Int J Biochem Cell Biol. 2022;147:106211.
93. Nuzzo AM, Giuffrida D, Zenerino C, Piazzese A, Olearo E, Todros T, Rolfo A. JunB/cyclin-D1 imbalance in placental mesenchymal stromal cells derived from preeclamptic pregnancies with fetal-placental compromise. Placenta. 2014;35(7):483–90.
94. McHugh CA, Chen CK, Chow A, Surka CF, Tran C, McDonel P, Pandya-Jones A, Blanco M, Burghard C, Moradian A, et al. The Xist lncRNA interacts directly with SHARP to silence transcription through HDAC3. Nature. 2015;521(7551):232–6.
95. Kim D, Langmead B, Salzberg SL. HISAT: a fast spliced aligner with low memory requirements. Nat Methods. 2015;12(4):357–60.
96. Li B, Dewey CN. RSEM: accurate transcript quantification from RNA-Seq data with or without a reference genome. BMC Bioinformatics. 2011;12:323.
97. Pertea M, Pertea GM, Antonescu CM, Chang TC, Mendell JT, Salzberg SL. StringTie enables improved reconstruction of a transcriptome from RNA-seq reads. Nat Biotechnol. 2015;33(3):290–5.
98. Soneson C, Love MI, Robinson MD. Differential analyses for RNA-seq: transcript-level estimates improve gene-level inferences. F1000Res. 2015;4:1521.
99. Vaiman D, Calicchio R, Miralles F. Landscape of transcriptional deregulations in the preeclamptic placenta. PLoS ONE. 2013;8(6): e65498.
100. Kleinrouweler CE, van Uitert M, Moerland PD, Ris-Stalpers C, van der Post JA, Afink GB. Differentially expressed genes in the pre-eclamptic placenta: a systematic review and meta-analysis. PLoS ONE. 2013;8(7): e68991.
101. Brew O, Sullivan MH, Woodman A. Comparison of Normal and Pre-Eclamptic Placental Gene Expression: A Systematic Review with Meta-Analysis. PLoS ONE. 2016;11(8):e0161504.
102. Kaartokallio T, Cervera A, Kyllonen A, Laivuori K, Kere J, Laivuori H, Group FCI. Gene expression profiling of pre-eclamptic placentae by RNA sequencing. Sci Rep. 2015;5:14107.
103. Kobayashi H. Characterization of the down-regulated genes identified in preeclampsia placenta. Hypertens Pregnancy. 2016;35(1):15–21.
104. Lambert SA, Jolma A, Campitelli LF, Das PK, Yin Y, Albu M, Chen X, Taipale J, Hughes TR, Weirauch MT. The Human Transcription Factors. Cell. 2018;172(4):650–65.
105. Heinz S, Benner C, Spann N, Bertolino E, Lin YC, Laslo P, Cheng JX, Murre C, Singh H, Glass CK. Simple combinations of lineage-determining transcription factors prime cis-regulatory elements required for macrophage and B cell identities. Mol Cell. 2010;38(4):576–89.
106. Yu G, Wang LG, Han Y, He QY. clusterProfiler: an R package for comparing biological themes among gene clusters. OMICS. 2012;16(5):284–7.
107. Yang X, Yang J, Liang X, Chen Q, Jiang S, Liu H, Gao Y, Ren Z, Shi YW, Li S, et al. Landscape of Dysregulated Placental RNA Editing Associated With Preeclampsia. Hypertension. 2020;75(6):1532–41.

Publisher's Note